4455-6002-RU000

SURVEY OF VLF ELECTRIC FIELDS IN THE MAGNETOSPHERE WITH THE POLAR ORBITING SPACECRAFT, 1964-45A

by

F. L. Scarf, G. M. Crook, and R. W. Fredricks

Space Sciences Laboratory
TRW Systems*
Redondo Beach, California

ABSTRACT

The VLF electrometer on the Lockheed-Aerospace P-11 satellite, 1964-45A, sampled ambient electric fields in the frequency range 1.7 - 14.5 kc/s. Tape recorded data for sixteen full orbits were obtained between 15 August 1964 and 13 September 1964. A complete description of the experiment is given and all of the results are displayed and analyzed. It is argued that the observed fields generally represent electrostatic plasma oscillations in the ambient medium, and various sources of the large nonequilibrium noise enhancements are considered. It is noted that d-c electric fields parallel to the geomagnetic field lines (possibly associated with the flute instability) could produce the large amplitude plasma oscillations and related phenomena.

Author

*Formerly TRW Space Technology Laboratories

1. INTRODUCTION

On August 15, 1964 the P-11 spacecraft 1964-45A carried into a near polar orbit an a-c electrometer capable of measuring VLF electric fields in the frequency range 1.7 to 14.5 kc/s. Recently Scarf, Crook, and Fredricks (1965; henceforth referred to as SCF) published a preliminary report on the electric field measurements in which it was argued that the instrument had detected large amplitude ion plasma oscillations. In this paper we present a comprehensive summary of the observations and assess the significance of the results.

Section II contains a description of the spacecraft orbit, the operation of the electrometer, the orientation of the antenna, and wake effects which supplements the discussion in SCF. The full data for sixteen tape-recorded orbits are displayed and discussed in Section III, and for eight orbits the field measurements are also correlated with observations of precipitating electrons having $E > 400$ kev. The total amount of data discussed is thus quite large, but since this experiment is the first of its kind it appears necessary to examine the measurements for many orbits in order to establish repetitive patterns and the range of variability. It is argued in Sections II, III that the instrument has not generally detected the electric field noise spectrum associated with the ion cyclotron resonance or harmonics, the hybrid resonances, shot noise, photoelectron emission, whistler signals, wake disturbances, or on-board interference. Sheath effects also appear to be insignificant, and it is therefore concluded that the measured fields represent electrostatic ion waves in the ambient plasma. Although the opportunities for comparison are quite limited, it is shown that the appearance of precipitating energetic electrons generally is correlated with the detection of enhanced plasma oscillation fields.

The significance of these observations is discussed in Section IV. The evidence suggests very strongly that the magnetosphere and upper ionosphere are in a state of marginal stability with respect to a generalized form of two-stream instability associated with an anisotropic velocity distribution, and various specific instabilities are considered. One class is related to a spatial anisotropy, and for the magnetospheric

parameters of interest this is typified by the Rosenbluth-Post "Loss-Cone" instability (1965) which occurs when particles are confined in a mirror geometry. The other class is the more familiar form of the two-stream instability associated with an energy anistropy which might be produced by a d-c electric field along the geomagnetic field lines (SCF, Swift, 1965a). Such a d-c field could arise if the magnetosphere were unstable with respect to fluting (Chang, Pearlstein, and Rosenbluth, 1965, Swift, 1965b) although other sources of $E_{||}$ are possible. The P-11 VLF data alone cannot be used to identify the source of the enhanced plasma oscillations, but additional evidence which seems to support the conjecture that large electric fields exist along geomagnetic field lines is summarized.

II. THE VLF EXPERIMENT

The orbit of spacecraft 1964-45A has apogee near 3765 km above the earth's surface and a perigee near 268 km, with an inclination of 96°. The initial perigee (August 15, 1964) was on the night side at a latitude near $+20^{\circ}$ (geographic) and at a local time near 1:40 a.m. Because of the eccentricity and inclination of this orbit, the normal precession in longitude associated with oblateness of the earth was almost canceled by that change associated with the movement of the earth around the sun, so that the spacecraft remained at nearly the same local time. However, as time passed, the orbital orientation did change in two ways: 1) a slight drift in local time occurred, and by 13 September 1964 the local time for perigee was reduced to 00:59 a.m.; 2) the perigee latitude steadily drifted southward crossing the geographic equator on 23 August 1964, and reached -41° by 13 September 1964. Thus, the principal parameters which change from orbit to orbit are the geographic longitude and the altitude at which a given geomagnetic or geographic latitude is crossed.

Real-time data were acquired as the spacecraft passed over certain tracking stations. The duration of these transmissions was generally on the order of 5 - 15 minutes, but since the VLF experiment was assigned only eight data points per 1.068 minutes, and since these transmissions were taken over a few specific geographical locations, it has not been deemed worthwhile to base an extensive analysis of the data on any of these limited real-time observations. The spacecraft did have on board a tape recorder which periodically allowed sampling of the fields for a complete

orbit, and our discussion will be based entirely on the tape recorded data. The real time data have been examined, however, and it has been verified that the tape recorded observations are quite representative of all of the measurements.

After about one month of operation a drift in the VCO frequency for the tape recorder channel involving our subcommutator points occurred, and only sporadic and somewhat noisy recordings were available thereafter. Furthermore, since the telemetry for our experiment was extremely limited, any noise in the link (such as temporary loss of synchronism during the tape playback) was frequently sufficient to degrade the entire recording. Therefore, only tape recorded data for sixteen orbits during the period 15 August 1964 to 13 September 1964 are available. Some relevant orbital parameters for these passes are summarized in Table 1. The orbits are labeled by the perigee pass number, as given in the standard ephemeris for 1964-45A. (Some data for orbits 48, 86 were shown in SCF, but in the earlier discussion the standardized numbering system had not been adopted, and these were described as orbits 47, 85 respectively.)

The payload of 1964-45A included a series of omnidirectional solid state particle detectors furnished by Drs. Freden, Paulikas, and Blake of the Aerospace Corporation (Freden, et al., 1965). These instruments measure fluxes of electrons with energies greater than 300 - 400 kev, and these electron observations were kindly made available to us. The omnidirectional detector responds to both trapped and precipitating energetic electrons, but the study of interest involves the relation between large electric fields and precipitating particles. For this reason we have confined examination of the Aerospace data to spatial regions where trapped electrons cannot exist. In Figures 2, 4, 6, 8, 10, 12, 14, 16, vertical lines are drawn to delineate the portions of the orbit where $B(L) > B_{min}(L)$ at an altitude of 100 km (curves of $B_{min}(L)$ for a variety of altitudes were supplied by Dr. J. Vette); in these regions no trapped electrons can exist, and the Aerospace electron fluxes therefore represent detection of precipitating particles. This comparison was possible only for orbits 5 through 102; the mechanical subcommutator for the output channel which contained the particle data developed a temporary malfunction

Table 1. Perigee Parameters for Tape Recorded Orbits

Perigee Number	Date	Geographic Latitude	L	Invariant Latitude	East Longitude	Universal Time	Local Time
5	15 Aug	17.47°	1.412	31.52°	281.34°	6:54	1:39
10	15 Aug	16.59°	0.995	9.37°	121.87°	17:31	1:38
21	16 Aug	14.67°	0.992	6.93°	131.04°	16:53	1:35
44	18 Aug	10.67°	0.967	3.03°	117.51°	17:44	1:34
48	19 Aug	9.94°	1.062	6.25°	349.94°	2:14	1:32
65	20 Aug	6.96°	1.010	0.80°	167.80°	14:21	1:31
86	22 Aug	3.19°	1.039	5.42°	218.02°	10:57	1:27
102	23 Aug	0.38°	1.005	7.45°	67.75°	20:56	1:26
157	28 Aug	-9.48°	1.114	19.83°	81.93°	19:51	1:19
167	29 Aug	-11.23°	1.117	21.30°	123.08°	17:06	1:19
202	1 Sept	-17.37°	1.288	28.58°	87.09°	19:25	1:13
207	2 Sept	-18.25°	1.095	2.17°	287.67°	6:02	1:11
217	3 Sept	-19.95°	1.185	11.66°	328.89°	3:16	1:10
262	7 Sept	-27.81°	1.313	19.78°	334.24°	2:50	1:08
267	7 Sept	-28.69°	1.498	35.39°	174.85°	13:27	1:06
339	13 Sept	-41.2 °	2.401	45.67°	39.97°	22:19	00:59

after orbit 147, and by the time this resumed operation the VCO drift had occurred.

As described in SCF, the experiment contains four bandpass channels (center frequencies 1.7, 3.9, 7.35, and 14.5 kc/s; bandwidth 15% of center frequency) plus an overcounter set to trigger at 1 volt/meter. The noise threshold is on the order 300 - 400 μv/m for the bandpass channels, with a dynamic range of 70 db. These field strengths are not actually absolute values. The antenna, a single whip of length 18 inches, mounted parallel to the spin axis of the spacecraft, is coupled to the preamplifier so that the antenna capacitance and the input capacitance of the preamplifier form a voltage divider. Thus, the excess charge or potential amplitude on the antenna is actually measured. We define the indicated field strength by $E_{ind}\, \ell_{eff} = \phi_o$, where $\ell_{eff} = \ell/2 = 0.23$ meters and ϕ_o is derived from the preamplifier input voltage using the free space antenna capacitance, $C_o \simeq 5.5$ picofarads. The ambient potential amplitude can differ from ϕ_o if the antenna capacitance in the plasma is not C_o, and E_{ind} may differ from the actual field strength because of any variation in the antenna capacitance and also because the effective length may differ from $\ell/2$. Neither of these uncertainties appears to be very serious. As we shall demonstrate in Section III, certain features of the data indicate that no well-defined insulating sheath formed around the antenna at the orbit of the spacecraft, and this, in turn, strongly suggests that C and ϕ were very near C_o and ϕ_o, respectively. The uncertainty in the effective length cannot be evaluated on the basis of the data, or on the basis of prelaunch calibration which involved external potentials rather than external electric fields. However, taking into account the known size of the spacecraft, it is difficult to see how the quoted effective length can be in error by more than 50%.

The spacecraft had on board several potential sources of VLF interference such as the 2 kc/s square wave generator for the Aerospace Corporation Faraday cup plasma probe, and one must consider the extent to which the VLF detector could be contaminated by these instruments. Extensive prelaunch integration tests revealed that the electric field experiment is completely insensitive to this kind of noise. In essence, the voltage

divider input circuit produces such a high impedance that magnetic oscillations cannot drive currents, while the ambient electric field interference levels are well below threshold for the experiment. Of course, tests such as these are carried out in the absence of plasma, and it is dangerous to ignore the possible effect of a plasma medium which allows new propagating, or even growing, modes of oscillation in the VLF range. For instance, one could imagine that the 2 kc/s generator might stimulate ion acoustic waves in the nearly collisionless plasma and that these local effects might contribute to the indicated field strengths in the 1.7 kc/s channel. Furthermore, at certain places in the orbit, on-board noise source frequencies match local resonance frequencies such as that of the lower hybrid resonance,

$$f \approx \sqrt{f_c^{\,i} f_c^{\,e}} \; ;$$

the resonance effects could be particularly important because the group velocity vanishes for these modes and large power levels can therefore be built up near the spacecraft. In fact, lower hybrid resonance emissions and the fundamental ion gyrofrequency resonance were detected on Injun III and on Alouette I (Brice and Smith, 1964; Brice et al., 1964; Smith, et al., 1964; Gurnett and O'Brien, 1964).

We feel that no spacecraft-stimulated emissions associated with the ion gyrofrequency resonance were found in this experiment. During a typical orbit the ambient magnetic field varies from about 0.05 gauss to 0.5 gauss and hence the proton gyrofrequency ranges from 76 c/s to 760 c/s. Since the supposed source of this emission (i.e., the spacecraft or its equipment) and the receiver are in the same frame of reference, such a signal can be detected only in a channel with significant response below 800 c/s. However, our lowest channel is centered at 1.7 kc/s, and the sustained average 800 c/s field amplitude would have to be greater than 1 volt/meter in order to be seen above background in the 1.7 kc/s channel. Such large coherent signals would have been detected in the overcounter channel, and the lack of overcounter response precludes this possibility.

The ion cyclotron harmonics with angular frequencies near $n\,\Omega_c$, $n = 2, 3, \ldots$ do have components which can fall in the range of 1.7 kc/s, but for the fields and densities encountered in the lower magnetosphere, these waves primarily represent bumps or ripples in the ordinary propagating ion wave spectrum. For example, the dispersion relations for $n = 2, 3$ are (Sturrock, 1965)

$$\omega^2 \simeq (2\,\Omega_c)^2 + \frac{\Omega_p^{\,2}\, k^2 A^2 \sin^4\theta}{2\,\Omega_c^{\,2} - \frac{1}{6}\,\Omega_p^{\,2}\,(4-\cos^2\theta)} + \ldots \qquad (1)$$

$$\omega^2 = (3\,\Omega_c)^2 + \frac{3\,\Omega_p^{\,2}\, k^4 A^4 \sin^6\theta}{32\,\Omega_c^{\,4} - \frac{4}{9}\,\Omega_c^{\,2}\,\Omega_p^{\,2}\,(9-\cos^2\theta)} + \ldots \qquad (2)$$

where $\frac{1}{2}\,M_p A^2 = KT_p$, $\Omega_p^{\,2} = 4\pi\,Ne^2/M_p$, $0 < k < K_D = 2^{\frac{1}{2}}\,\Omega_p/A$ and $\vec{k}\cdot\vec{B} = kB\cos\theta$. If $\Omega_p^{\,2}/\,\Omega_c^{\,2}$ is not large, then the "resonances" are narrow and the k-dependence is unimportant. This condition is indeed satisfied for magnetospheric electrons, and sharp electron gyrofrequency harmonic resonances were detected on Alouette I (Fejer and Calvert, 1964; Sturrock, 1965). However, when ions are considered the situation is completely different since $\Omega_p \sim M^{-1/2}$ while $\Omega_c \sim M^{-1}$, and the dispersion relations describe modes with a very different character. When $\Omega_p >> \Omega_c$ (as it is for magnetospheric protons) the broad-band spectrum extends from 0 to $(n\,\Omega_c)$ and the phase and group velocities are sizeable. Thus, these harmonic cyclotron "resonances" are merged with the ordinary ion wave background where the dispersion relation for parallel ion wave propagation ($\vec{k} \times \vec{B} = 0$) is

$$\frac{1}{\omega^2} \simeq \frac{M_p}{k^2 KT_e} + \frac{1}{\Omega_p^{\,2}}\,, \quad 0 < k < K_D\,. \qquad (3)$$

It will be shown in the next section that isolated single, or perhaps double channel peaks have been detected on occasion. It is conceivable that some of these represent emissions at the lower hybrid resonance frequency ($f \simeq 63$ B kc/s for a hydrogen plasma, where B is in gauss). However, a cursory examination of the magnetic field values at these spikes (discussed in the text of Section III) shows that very few of these can possibly be related to lower hybrid emissions for protons or heavier ions.

Another general point which must be discussed involves the orientation of the electric field antenna with respect to the spacecraft velocity vector. The spacecraft traveled from south to north on the night side and the antenna pointed within 15° of north. Thus the antenna was generally out of the wake on the night side, but it is necessary to consider the extent to which the measurements were distorted by the motion through the plasma.

The most extensive investigation of wake effects and local distortions was carried out by Samir and Willmore (1965) on Ariel. The payload included Langmuir probes which directly measured electron densities and indirectly detected VLF electric fields in the range 2.7 - 3.7 kc/s via the relation $\vec{\nabla} \cdot \vec{E} = 4\pi\rho$. One probe was mounted on the spacecraft and the other on a 57-inch boom. It was found that the boom probe response was completely unaffected by its orientation with respect to the spacecraft wake, suggesting a wake extension of less than a few feet. The base probe did show that a small wake region depleted of plasma exists, and when the total density was down (i.e., when the base probe pointed in the wake) flux oscillations were detected. Samir and Willmore speculated that ion plasma waves were excited in the wake region. Another possible interpretation of their result is that when most of the steady plasma component is swept out, the part which arrives at the base probe has a higher percentage fluctuation amplitude; this could mean that the weak density oscillations are present throughout the plasma, but only observable on Ariel when the base probe points in the depleted region. At any rate, the Ariel measurements strongly suggest that when the VLF antenna points upstream (on the night side) it samples fields in a plasma which is relatively undisturbed.

III. TAPE RECORDED DATA

The telemetry sequence for the VLF experiment was the following: The bandpass channels were sampled in the order 1.7, 3.9, 7.35, plus voltage calibration, 14.5, 7.35, 3.9, 1.7 kc/s, with one second between points and 1.068 minutes between each sequence. Thus the 1.7, 3.9, and 7.35 kc/s channels were sampled twice per sequence, with 7, 5, and 3 seconds, respectively, between samples. The results are displayed in Figures (1) - (32) and the format is similar to that used in SCF. For the three low frequency channels the first sampling in each sequence is plotted without a heavy dot and successive first samplings are connected; the vertical lines leading to points with heavy dots then show the variations in field levels over 7, 5, or 3 seconds. For each of the sixteen tape-recorded orbits two graphs are provided. One shows the complete response in all four bandpass channels, and the other contains only the 1.7 kc/s measurements along with ephemeris parameters and Aerospace Corporation electron data, where available. It is useful to discuss the results for each orbit individually:

Orbit 5 (See Figures 1, 2): The spacecraft entered shadow at 6:34 UT, and signal was lost before it emerged. A slight but significant noise enhancement appeared in all four channels as the photoflux disappeared, and this could be taken as an indication that a sheath formed at about 6:34 UT, causing an apparent field enhancement as discussed in SCF. However, it will be seen that the measured fields generally show no change at all when the spacecraft crosses the terminator, and it seems likely that a normal moderate noise enhancement was coincidentally simultaneous with entrance into the shadow. This orbit is the only one in which no fields higher than 6 millivolts/meter were measured; it is also the only one available for comparison in which no precipitating electrons were detected.

Orbit 10 (See Figures 3, 4): The spacecraft was in shadow between 17:11 UT and 17:40 UT. The first passage across the terminator occurred during a quiet portion of the orbit, and clearly no change in the indicated field level was measured. This strongly suggests that no sheath corrections are required at any time since the sheath should be modified drastically when the photoflux is turned off. The most prominent feature of this orbit is the large field enhancement between 17:35 UT and 17:46 UT which appears to be correlated in a complex manner with observation of precipitating energetic electrons at the spacecraft, and at the conjugate region some 30 - 40 minutes earlier. This four-channel noise increase occurred over an altitude range of 300 - 950 km with $B \simeq 0.41 - 0.46$ gauss and $L \simeq 1.2 - 8$; the field peaks were found at $L \simeq 1.4$, 2.1, 6, and some sort of anti-correlation between the field strength and the particle flux seems to be established. However, the extremely limited telemetry available for the VLF experiment and the lack of vector measurements precludes a detailed study of this relation (See also Orbits 21, 48, 86, 102.)

Orbit 21 (See Figures 5, 6): The spacecraft was out of shadow between 17:02 UT and 18:41 UT. Since the terminator crossings coincided with the start of an enhancement and with loss of signal, no statements about sheath effects can be derived from these measurements. As before, the prominent four-channel enhancement from 17:01 UT to 17:11 UT has a dip which appears to be related to the detection of large fluxes of precipitating electrons. The first peak at 17:01 to 17:04 UT has $L \simeq 450$ to 650 km, $B \simeq 0.44$ to 0.43 gauss, and $L \simeq 1.6 - 3.2$, and the second at 17:06 to 17:11 UT has $L \simeq 740$ to 1150 km, $B \simeq 0.35$ to 0.42 gauss, and $L \simeq 4 - 16$. At the second night side auroral pass the signal was frequently missing, but some indication of high field strengths was obtained. For orbits 10, 21 the VLF electric field signals were also compared with the response of Aerospace Corporation Faraday cup plasma probe (Hilton, Stevens, and Vampola, 1964). General agreement was found between the uniaxial field measurements and the detection of fluxes of 1 - 8 kev protons; the agreement was best on the night side where the VLF antenna was out of the spacecraft wake.

Orbit 44 (See Figures 7, 8): The spacecraft was in shadow between 17:26 and 17:45 UT. As it entered the shadow, the indicated fields again remained fairly smooth. The four-channel enhancements at t $\simeq$ 17:32 - 17:36 UT (L $\simeq$ 500 - 800 km, B $\simeq$ 0.44 gauss, L $\simeq$ 1.8 - 3.5) and 17:45 - 17:58 UT (L $\simeq$ perigee to 800 km, B $\simeq$ 0.35 - 0.45, L $\simeq$ 1 - 4) may be related to the adjacent observations of precipitating energetic electrons; however, the intermittent loss of synchronism between 17:52 UT and 18:02 UT makes any comparison rather poor for this pass. The isolated signal spikes at 17:16 - 17:19 UT (L $\simeq$ 2100 - 1800 km, B $\simeq$ 0.24 - 0.29 gauss, L $\simeq$ 10 - 30 with $L_{peak} \simeq 20$) and 18:38 - 18:41 UT (L $\simeq$ 3650 km, B $\simeq$ 0.09 gauss, L $\simeq$ 1.75) were both detected on the day side.

Orbit 48 (See Figures 9, 10): The spacecraft was in shadow between 1:56 UT and 2:24 UT. Again, the first passage across the terminator revealed no sharp change in the indicated field strengths. The four-channel enhancements at 2:20 to 2:25 UT (h $\simeq$ 360 - 650 km, B $\simeq$ 0.35 - 0.38 gauss, L $\simeq$ 1.4 - 3.8) and 2:29 to 2:34 UT (h $\simeq$ 900 - 1350 km, B $\simeq$ 0.37 - 0.33 gauss, L $\simeq$ 12 - 30) have the structure seen on orbits 10, 22; large electron fluxes are found at the dip between successive spikes, however, it is not certain that these electrons observed in the northern auroral zone are actually precipitating. The large electron flux measured between 1:52 and 2:06 UT must primarily represent trapped particles (this orbit passes over the magnetic anomaly). It is noteworthy, however, that a significant two-channel rise at 2:06 to 2:08 UT (h $\simeq$ 370 - 515, B $\simeq$ 0.24 gauss, L $\simeq$ 1.3) appears to be associated with the edge of the radiation belt. The isolated spikes at 1.53 UT and 3:07 UT have h $\simeq$ 1500 km, B $\simeq$ 0.26, L $\simeq$ 7.3, and h $\simeq$ 3600 km, B $\simeq$ 0.09 gauss, and L $\simeq$ 1.52, respectively. This pass is of interest because quite moderate fields were measured when the antenna encountered both the highest density at perigee, and the highest flux of trapped particles near apogee (see also Figure (6), SCF). Thus, it is highly unlikely that shot noise in the antenna contributes significantly to the indicated noise fields.

Orbit 65 (See Figures 11, 12): The spacecraft was in shadow between 14:03 UT and 14:31 UT, and the first passage across the terminator was roughly coincident with a moderate decrease in the background field intensity. Since the hypothetical night side sheath formation should result in an increase in the indicated field strength, these observations also support the contention that no sheath corrections are required. The broad four-channel noise increase at 14:14 UT to 14:20 UT appears to be associated with passage through the ionosphere ($h \simeq 418$ km to perigee, $B \simeq 0.3 - 0.38$ gauss, $L \simeq 1 - 1.3$). In the northern auroral region there was considerable loss of signal, but the four-channel data appear to indicate that a significant noise enhancement was present between 14:28 UT and 14:38 UT ($h \simeq 430$ km to 1100 km, $B \simeq 0.34$ to 0.37 gauss, $L \simeq 1.4 - 8$); it would seem that these results are not inconsistent with those obtained on orbits 10, 21, 48, with respect to the relation between VLF field strengths and precipitating electron observations, but the electron fluxes in the southern region are clearly unrelated to our measurements of E parallel to the spin axis.

Orbit 86 (See Figures 13, 14): This orbit during a magnetically quiet period is unique in several respects. The 76 millivolt/meter field is the largest seen in the normal channels during the lifetime of the experiment; the night side noise enhancements and the precipitating electron fluxes extend over an enormous region, and on the northern night side auroral pass the 3.9 and 7.35 kc/s noise signals are consistently more intense than the 1.7 kc/s fields. The first large enhancement in the two lowest frequency channels at 10:34 to 10:41 UT occurs at an altitude range of 1000 - 1650 km ($B \simeq 0.28 - 0.36$ gauss, $L \simeq 3.3 - 9.5$). The 76 millivolt/meter peak at 10:39 has $h \sim 1200$ km, $B \simeq 0.34$, $L \simeq 4.6$, and the remaining part of this large noise signal (to 10:41 UT) appears to be coincident with a dip in electron flux. As in orbits 10, 21, and 48, the subsequent dip in field strength (10:42 - 10:44 UT) occurs where the electron flux peaks. Near perigee the relation between E and J_e is not clear. The huge electron fluxes at low altitudes between 10:52 and 11:05 UT are accompanied by significant rise in the 3.9 and 7.35 kc/s fields, and between 11:12 and 11:20 UT ($h \simeq 920 - 1600$ km, $B \simeq 0.37 - 0.30$ gauss,

$L \simeq 4.9 - 20$) exceptionally large fields are found in all high frequency channels, but only moderate signals occur at 1.7 kc/s. In this connection, it is perhaps worth stressing again that this VLF experiment is only capable of measuring the component of E parallel to the spin axis.

The indicated field strength is actually a one-second average derived by multiplying the measured potential amplitude by the idealized effective length, $\ell_{eff} \simeq 0.23$ meter. For this kind of noise, the true peak potential, ϕ_p, must be at least three times the indicated average, and thus the 76 millivolt/meter measurement implies $e\phi_p > 52$ millivolts. Since the electron thermal energy is only about 170 millivolts at $h \simeq 1200$ ($T_e \simeq 2000^{\circ}k$), $e\phi_p$ exceeds 0.3 kTe, which is close to the theoretical maximum (see SCF). If this deduction is correct, we might expect to see very short wavelength fields with much larger magnitudes; i.e. $E_p \sim K_D \phi_p$ where K_D is the Debye wavenumber. Thus, if $K_D^{-1} \sim 1$ cm, $\phi_p \sim 50$ millivolts, $E_p \simeq 5$ volts/meter. In fact, these large amplitude short wavelength fields may have been detected on occasion in the P-11 overcounter channel. As mentioned in SCF, the overcounter was set to trigger at a threshold of 1 volt/meter. Although the frequency of a continuous coherent large amplitude signal would be indicated in this channel, a short duration pulse would merely produce an output to signify that the signal had been received. Overcounter responses of the latter type were found from time to time, but no large amplitude signals of sufficiently long duration were ever detected. This suggests strongly that any fields with $E > 1$ volt/meter had $\lambda \ll \ell_{eff}$ so that the conditions for constructive interference on the "long" antenna were only established momentarily.

Orbit 102 (See Figures 15, 16): On this pass the perigee occurred near the geographic equator and hence the antenna pointed in the direction of motion over a large portion of the night side pass. Because of the symmetry, the terminator crossings occurred near the active auroral or polar zones (shadow between 20:40 UT and 21:08 UT). The rather strong spike at 20:39 UT to 20:41 UT ($h \simeq 900 - 1100$ km, $B \simeq 0.36 - 0.37$ gauss, $L \simeq 8.6 - 26$) might appear to be related to the next enhancement at 20:46 to 20:50 UT ($h \simeq 370 - 600$ km, $B \simeq 0.36 - 0.37$ gauss, $L \simeq 1.5 - 3$) to

form a double peak structure as in orbits 10, 21, 48, and 85, and some precipitating electrons are actually found in the dip region between 20:41 and 20:46 UT. However, the possible relations are not clearly defined by these uniaxial field measurements, and the severe telemetry limitations also restrict the interpretation. The more moderate broad rise between 21:00 and 21:10 UT ($L \simeq 320$ km to 900 km, $B \simeq 0.34 - 0.37$ gauss, $L \simeq 1 - 3.4$) may also have a double peak structure.

Orbit 157 (See Figures 17, 18): The spacecraft entered the shadow at 19:38 UT and emerged at 20:06 UT. There were no sudden changes in the indicated fields as the spacecraft entered shadow, but as it was emerging the instrument appeared to detect the fairly common dip between successive peaks. This structure at 20:02 - 20:10 UT was found at $L \simeq 1.3 - 3.8$, $h \simeq 500 - 1200$ km, $B \simeq 0.37 - 0.34$ gauss. The most prominent feature of this record is obviously the very strong four-channel enhancement near perigee ($t \simeq 19:47 - 19:52$ UT, $h \simeq 360 - 275$ km, $B \simeq 0.43 - 0.36$ gauss), but the moderate three-channel dayside peak at 20:26 - 20:30 UT ($h \simeq 2500 - 2800$ km, $L \simeq 80 - 14$ with $L_{peak} = 20$, $B \simeq 0.22 - 0.20$ gauss) is also noteworthy. For this orbit and the remaining ones no electron data are available.

Orbit 167 (See Figures 19, 20): The spacecraft entered the shadow at 16:52 UT and emerged at 17:51 UT. Once again, there were no sudden changes in the indicated fields associated with a change in the photoflux. The 1.7 kc/s response was relatively quiet; however, a somewhat unusual four-channel enhancement occurred between 17:00 and 17:05 UT (altitude range 400 km to perigee, $B \simeq 0.5 - 0.4$ gauss), and an enhancement appeared primarily in the mid-frequency channels at 16:56 - 16:59 UT ($h \sim 615 - 450$ km, $B \sim 0.49 - 0.51$ gauss, $L \sim 6 - 3$). The largest 1.7 kc/s rise at 17:22 - 17:27 UT was found at an altitude of 1000 - 1400 km ($B \sim 0.36 - 0.31$ gauss, $L \sim 2.6 - 5.3$).

Orbit 202 (See Figures 21, 22): The spacecraft was in shadow between 19:13 and 19:42 UT, and the first passage across the terminator clearly shows that no sheath corrections influence the indicated field levels. The first four-channel noise increase at 19:22 to 19:30 is

again associated with passage through the ionosphere ($h \simeq 350$ km to perigee, $B \simeq 0.45 - 0.33$ gauss, $L \simeq 1 - 2.2$) and the night side auroral enhancement at 19:38 - 19:48 UT ($h \simeq 740 - 1600$ km, $B \simeq 0.29 - 0.35$ gauss, $L \sim 1.3 - 6.2$) is quite moderate. The day side spike is at 20:05 to 20:10 UT ($h \simeq 2930 - 3200$ km, $B \simeq 0.16 - 0.19$ gauss, $L \simeq 7.6 - 25$). Such signals were seen more frequently in these later passes as perigee drifted southward.

Orbit 207 (See Figures 23, 24): The terminator crossings occurred at 5:50 UT and 6:19 UT, but the fields were moderately disturbed at both times and nothing can be stated concerning sheath effects. The extremely large enhancements between 6:00 and 6:12 UT are clearly ionospheric ($h \simeq 350$ km to perigee, $B \simeq 0.24 - 0.36$ gauss, $L \simeq 1.2 - 1.6$); it is worth noting that the individual peaks are not symmetric about perigee (at 6:02 UT, $h = 276$ km, $B = 0.237$ gauss, while at 6:075 UT, $h = 343$ km, $B = 0.295$ gauss). There is some evidence for a very moderate noise increase in the northern auroral zone, but the large signals at 6:24 UT to 6:29 UT are clearly polar ($h \simeq 1500 - 1900$ km, $B \simeq 0.32 - 0.27$ gauss, $L \simeq 18 - 124$). The isolated 7.35 kc/s 22.1 millivolt/meter signal was detected at an altitude of 3490 km, with $B = 0.11$ gauss, $L = 1.64$.

Orbit 217 (See Figures 25, 26): On this relatively quiet pass the spacecraft entered shadow at 3:05 UT and emerged at 3:34 UT; again no sharp changes in indicated field levels are associated with these times. The four-channel enhancement at $t \simeq 3:08 - 3:17$ UT had $h \simeq 542$ km to perigee, $B \simeq 0.27 - 0.22$ gauss. The auroral enhancement at $L \simeq 6 - 7$ occurred mainly in the 3.9 and 7.35 kc/s channels ($t \simeq 2.59 - 3:05$ UT, $h \simeq 1200 - 730$ km, $B \simeq 0.35 - 0.31$ gauss) and the parameters for the isolated 3.9 kc/s peak at 3:40 UT are $h \simeq 1650$ km, $B \simeq 0.29$ gauss, $L \simeq 22$.

Orbit 262 (See Figures 27, 28): This complex recording was taken during the early hours of a moderate geomagnetic disturbance and several kinds of noise bursts were detected. The terminator crossings occurred at 2:40 and 3:09 UT and the enhancement between 2:42 and 2:55 UT is clearly ionospheric ($h \simeq$ perigee to 500 km). Perhaps the most interesting events are the day side auroral enhancements at 2:17 to 2:25 UT

(h $\simeq$ 1740 to 2470 km, B $\simeq$ 0.2 - 0.31 gauss, L $\simeq$ 2.7 - 11.7; large fields in the higher frequency channels only) and at 3:33 to 3:36 UT (h $\simeq$ 3140 - 3340 km, B $\simeq$ 0.15 - 0.17 gauss, L $\simeq$ 4.2 - 6.4; primarily 1.7 kc/s noise). The 1.7 kc/s spike at 3:13 - 3:15 UT was detected at an altitude of 1600 - 1800 km with B $\sim$ 0.28 gauss and L $\simeq$ 8 - 18.

Orbit 267 (See Figures 29, 30): These data represent the only measurements taken while a moderate geomagnetic storm was in progress, and all four passes through the auroral regions show some noise enhancement. On the first daylight pass at 12:05 to 12:07 UT (h $\simeq$ 3275 - 3410 km, B $\simeq$ 0.15 gauss, L $\simeq$ 4.7 - 6.3) a very modest field rise is apparent. The southern pass occurs some 60 minutes later and at a completely different altitude (for t between 13:06 and 13:12 UT, h $\simeq$ 900 - 1460 km, B $\sim$ 0.24 - 0.39 gauss, L $\sim$ 4 - 10.5) and this traversal is marked by the unique detection of sustained high fields in the 3.9 kc channel. (It should be apparent that most noise enhancements detected on 1964-45A have a very different character involving large fluctuations from high to near background levels.) The lack of any simultaneous activity in the 1.7 kc/s and 14.5 kc/s channels is quite unusual (however, see orbits 86, 217). On the next (night-side) auroral pass at 13:15 to 13:20 UT (h $\simeq$ 420 - 750 km, B $\simeq$ 0.44 - 0.51 gauss, L $\simeq$ 4.4 - 12.9) the enhanced noise does appear in all four channels, and a more moderate four-channel rise is again present at 13:47 - 13:53 UT (L $\simeq$ 1340 - 1940 km, B $\simeq$ 0.26 - 0.28 gauss, L $\simeq$ 2.1 - 5.9). The characteristic broad perigee rise in field level was again detected, and the isolated 1.7 kc/s spike at 13:21 - 13:24 UT occurred at an altitude of 300 - 407 km with B = 0.49 - 0.51 gauss and L = 2 - 4. The terminator crossing times were 13:17 and 13:47 UT.

Orbit 339 (See Figures 31, 32): The spacecraft was in shadow between 22:12 UT and 22:43 UT. Because the perigee had precessed so far to the south, the entrance into shadow, the approach to perigee, and traversal of high L-values coincide on this pass. The prominent four-channel enhancement at t $\simeq$ 22:10 - 22:20 UT occurred for h $\simeq$ 550 km - perigee, L $\simeq$ 26 - 2.4, B $\simeq$ 0.44 - 0.3 gauss, but the peak fields were measured at L = 4 - 6. The other night side enhancements were detected

only in the 1.7 kc/s channel. For t $\simeq$ 22:28 - 22:33 UT, h $\simeq$ 500 - 850 km, B $\simeq$ 0.26 - 0.24 gauss and L $\simeq$ 1.1, while for t $\simeq$ 22:44 - 22:46 UT, h $\simeq$ 1700 - 2000 km, B $\simeq$ 0.23 gauss and L $\simeq$ 3 - 5. The day side enhancement at t $\simeq$ 23:00 - 23:05 UT had h $\simeq$ 3000 - 3300 km, B $\simeq$ 0.19 - 0.17 gauss and L $\simeq$ 390 - 34.

Later Orbits: After approximately 400 orbits the VCO drift occurred and only a few useful conclusions can be derived from the subsequent measurements. In particular, late in November, 1964, the orbit had precessed sufficiently so that apogee was on the night side, with the antenna out of the spacecraft wake. Several fragmentary recordings reveal the following features: 1) The background field levels in all four channels generally remained near 1 - 2 millivolts/meter, but on occasion the instrument noise level (317 - 400 microvolts/meter) was detected simultaneously on all four channels. (These very low field strengths were never measured during the period 15 August to 13 September.) 2) The double-hump structure in the 1.7 kc/s channel was again found when the spacecraft passed through the radiation belts near apogee. The persistent form of this profile suggests that wake effects introduce no new oscillations, but merely change the coupling between the antenna and the ambient plasma. 3) Relatively intense isolated noise bursts were seen more frequently in the mid-frequency channels during these later passes.

IV. DISCUSSION

The most important results of the VLF electric field experiment or 1964-45A involve the measurements of sustained background field levels with E ~ 1 - 2 millivolts/meter in all channels, the detection of frequent and persistent enhancements with E(1.7 kc/s) $\simeq$ 20 - 75 millivolts/meter, and the observation that an abrupt change in the photoflux is not generally associated with a change in field level.

The customary smoothness of the field contours in the region of the terminator indicates that local field enhancement associated with the plasma sheath (SCF; Hall, Kemp, and Sellen, 1964) is minimal, and this in turn implies that the discussion in SCF based on correction factors of 0.33 to 0.2 was much too conservative. That is, the disparity

between the measured background field strengths and those anticipated on the basis of $E = cB/n$, where $B \leq 10^{-3}\ \gamma$ and $n \simeq 50$ ($f = 1.7$ kc/s), now appears to be at least two to two and one-half orders of magnitude, rather than the factor of 60 quoted in SCF. We again conclude that most of the measurements represent detection of short wavelength electrostatic oscillations.

The apparent background amplitude is, in fact, somewhat higher than the minimum or equilibrium value of E calculated in SCF using the Rostoker (1961) formula

$$\frac{E^2}{8\pi} = \frac{1}{(2\pi)^3} \int d^3k \, \frac{KT_e}{2} \, \frac{K_D^2}{(k^2+K_D^2)} \quad , \tag{4}$$

even when Doppler broadening is taken into account. Several natural explanations for this difference are available. For example, the collisionless plasma in the geomagnetic dipole field should have a velocity distribution which is anisotropic because of the existence of a loss cone. For $\Omega_p \ll \Omega_c$ a very moderate spatial anisotropy gives rise to the Harris type of instability (1961), which is essentially of the two-stream variety producing growing electrostatic resonances at $\omega = n\,\Omega_c$. However, for $\Omega_p \gg \Omega_c$ (as in the magnetosphere), this instability is transformed and growing ion acoustic waves are produced with a peak near the ion plasma frequency (Rosenbluth and Post, 1965).

The discussion of individual orbits in Section III shows that the enhanced fields occur at a great variety of altitudes, latitudes, and geomagnetic field values; however, several general geophysical regions along the polar orbit appear to be favored sources for this kind of activity. Specifically, greatly enhanced noise levels are frequently encountered in the upper ionosphere ($h \simeq 270$ - 500 km), near the auroral regions ($L \simeq 4$ - 8), and near the poles ($L > 12$). The peak noise strengths are generally much greater on the night side than in sunlight, and the enhanced field values exhibit very rapid amplitude fluctuations, rather than sustained high levels.

The fact that the enhanced noise fields appear as a sequence of bursts is consistent with the conjecture that the upper ionosphere and the magnetosphere are near some state of marginal stability with respect to production of plasma oscillations. That is, instabilities generally have self-quenching characteristics so that they become stabilized near marginal stability some time after triggering, allowing subsequent repetitions of the triggering sequence. (See, for instance Figure (8) in SCF.) In order to test this conjecture we note that slow, short wavelength electrostatic oscillations can produce high energy electrons and protons via a gyrofrequency resonance (Fredricks, et al., 1965; Fredricks, 1965) and hence if the measured fields represent ion waves, we should expect to find bursts of high energy particles in similar regions. Indeed, recent observations of $E > 40$ kev electrons (McDiarmid and Burrows, 1965) and $E > 180$ ev electrons (Sharp, et al., 1965) do reveal a structure composed of narrow intense spikes, and X-ray emissions from auroral regions (Brown, et al., 1965) also have the nature of separate outbursts. In fact, studies of auroral energy spectrums in the range $E \sim 4$ - 100 kev (Westerlund, et al., 1965; Laquey, et al., 1965) show extremely large and rapid fluctuations in the spectral characteristics.

A full identification of the source of the field enhancements requires much more information than is available from the uniaxial VLF experiment alone. For instance, in the upper ionosphere where collisions might still be significant the large field strengths could be produced by electrons streaming across geomagnetic field lines via the collisional instability discussed by Buneman (1963) and Farley (1963). However, these perigee enhancements could also be produced by a runaway phenomenon associated with the presence of d-c electric fields parallel to the geomagnetic field lines. There is some evidence to support the second interpretation. Perkins, et al. (1965) recently detected the presence of weakly damped or enhanced electron plasma oscillations at $h \sim 150$ - 600 km using incoherent backscatter of the Arecibo radar signal. The enhanced levels above 300 km revealed that fast electron streams were radiating non-thermal plasma oscillations by the Cerenkov mechanism; the generation of both electron and ion plasma oscillations

is a characteristic of the runaway process, but not of the Buneman-Farley instability.

Similarly, we must turn to other measurements to interpret the large auroral and polar noise signals. Once again recent observations of a-c field levels at $f = f_p^e$ suggest that d-c electric fields parallel to geomagnetic field lines induce runaway. Huguenin, et al. (1964) found very large electric field bursts at 0.7 Mc/s in a region where $f_p^e \simeq$ 0.7 Mc/s and Scarf and Fredricks (1965) interpreted this as a direct measurement of the ambient electrostatic wave. On Electron -2, Benediktov et al. (1965) found sporadic electric fields at 0.725 Mc/s which were more than two orders of magnitude above the "cosmic" background. These generally had the "character of separate outbursts" and they were "well correlated with the appearance of flows of low energetic electrons ($E > 100$ ev)". Finally, O'Brien (1964) has shown that certain features of the Injun 3 electron measurements are consistent with the assumption that splashy precipitation is caused by temporary d-c electric fields parallel to $\vec{B}$ at high altitudes, and Swift (1965 a, b) has discussed this interpretation in some detail.

A possible source of magnetospheric electric fields along the geomagnetic field lines is associated with the flute instability. Swift (1965 b) considered a dynamical mechanism for magnetospheric charge separation electric fields in which particle injection on the day side of the magnetosphere, and particle losses on the day and night side combine to maintain a higher dayside population of trapped particles. It was suggested that the asymmetric ring current is unstable with respect to fluting and that thermal energy in the ring current is converted into plasma streaming which leads to auroral breakup, primarily on the night side.

A general discussion of the natural stability of the quiescent axially symmetric magnetosphere with respect to fluting was also recently presented by Chang, et al. (1965). Using the zero temperature conductivity tensor, the Liemohn and Scarf (1964) electron density distribution, $N_e(r) \sim r^{-3}$, and their estimate of a low electron temperature, it

was concluded that ionospheric current systems can readily stabilize the flute on the day side, but that the night side conductivity is such that the magnetosphere might be near marginal stability at all times. In fact, there are several reasons for believing that these stabilization calculations are overly optimistic: 1) The zero temperature conductivity is certainly an overestimate because plasma oscillations are readily generated in a warm plasma and these waves limit the current flow. In low density laboratory experiments the flute has never been stabilized by inserting grounded conducting end plates alone (W. Bernstein, private communication) and the question of stabilization by a low density conducting plasma is still open; 2) the whistler-derived density profile may be much closer to r^{-4} than to r^{-3} (D. Carpenter, private communication), and Swift (1965 b) has noted that the r^{-4} decrease is essentially one of marginal stability; 3) Chang et al. assumed $N_e \sim r^{-3}$ throughout the magnetosphere whereas the whistler analysis of Liemohn and Scarf only covered the range $2R_e < r < 4.5\ R_e$. However, as Swift pointed out, any discontinuity in the distribution could produce an overstability. Actually, there is considerable evidence for the existence of such a discontinuity near $L \simeq 4 - 8$ from analysis of "knee" whistlers (Carpenter, 1963; also private communication). Indeed, the existence of a permanent, but moveable "knee" in the distribution may be taken as an indication that a more or less continuous instability controls the loss of magnetospheric plasma; 4) Chang et al. assumed that the magnetospheric plasma is relatively cold, but Serbu (1964) found that the fraction of "hot" to "cold" electrons rises rapidly in the outer magnetosphere.

Other evidence for the dumping of soft electrons just beyond the 40 kev electron trapping boundary was recently presented by Fritz and Gurnett (1965), and all of these facts suggest that flute instabilities do limit the content of the magnetosphere and generate d-c electric fields along magnetic field lines. These in turn can then produce large amplitude plasma oscillations, superthermal particles (via the cyclotron resonance mechanism), and ultimately the aurora. However, the above conclusions are quite tentative, and considerable caution must be exercised in interpreting the observations. It has been pointed out

(Bernstein et al. 1965) that very similar phenomena are observed not only in the flute unstable low density laboratory mirror machines (Phoenix IA at Culham, Alice at Livermore, and Ogra at Moscow) but also in the flute stabilized devices (DCX I and II at ORNL and the stabilized Alice and Ogra). In all of these experiments $\Omega_c > \Omega_p$ and $\omega_p \geq \Omega_c$, so that spatial anisotropies produce electrostatic cyclotron resonances rather than ion waves, and these modes are indeed observed as a series of discontinuous bursts which occur in association with production of high energy protons and precipitation of electrons and protons with large $v_{||}$. The similarity between the flute stable and unstable devices with respect to bursts of electrostatic waves, acceleration, etc., suggests that these phenomena are produced in association with a plasma instability which is not driven by the flute. Moreover, even for the flute-stabilized devices, significant evidence for the existence of large d-c electric fields along the magnetic field lines is available, but the origin of these parallel fields is not understood (Bernstein, 1965).

ACKNOWLEDGMENTS

The data analysis and experiment construction was sponsored by the TRW Systems Independent Research Program and carried out by the Space Sciences Laboratory of the Physical Research Division; one of the authors (Scarf) has been supported by the National Aeronautics and Space Administration under Contract NASw-1226.

We are especially indebted to Dr. G. A. Paulikas of the Aerospace Corporation for his helpful cooperation throughout this program and to Drs. Paulikas, S. C. Freden, and J. B. Blake for their generosity in making available to us the energetic electron data. We are also grateful to Dr. R. S. White for the invitation to place the experiment on the satellite and to Dr. J. Vette for furnishing the curves of B_{min} (h, L).

We have benefited from discussions with Drs. L. R. O. Storey, R. A. Helliwell, D. L. Carpenter, H. H. Hilton, J. R. Stevens, J. W. Dungey, and D. W. Swift, and the valuable advice and suggestions of W. Bernstein are acknowledged with pleasure.

REFERENCES

Benediktov, E. A., G. G. Getmantsev, N. A. Mitjokov, V. O. Rapoport, J. A. Sazonov, and A. F. Tarasov, Intensity measurements of radiation at frequencies 725 and 1525 kc/s, by means of the receiver on the satellite "Electron-2", 1965 COSPAR preprint.

Bernstein, W., E. G. Murphy, M. Petravic, and D. R. Sweetman, Acceleration of protons during the ion cyclotron instability, Nature, May 22, 1965.

Bernstein, W., to be published, 1965.

Brice, N. M. and R. L. Smith, A very-low-frequency plasma resonance, Nature, 203, 926-927, 1964.

Brice, N. M., R. L. Smith, J. S. Belrose, and R. E. Barrington, Triggered very-low-frequency emissions, Nature, 203, 927, 1964.

Brown, R. R., J. R. Barcus, and N. R. Parsons, Balloon observations of auroral zone X-rays in conjugate regions, 2, microbursts and pulsations, J. Geophys. Res., 70, 2599 - 2612, 1965.

Buneman, O., Excitation of field aligned sound waves by electron streams, Phys. Rev. Letters, 10, 285 - 287, 1963.

Carpenter, D. L., Whistler evidence of a "knee" in the magnetospheric ionization density profile, J. Geophys. Res., 68, 1675 - 1682, 1963.

Chang, D. B., L. D. Pearlstein, and M. N. Rosenbluth, On the interchange stability of the Van Allen belt, J. Geophys. Res., 70, 3085 - 3098, 1965.

Farley, D. T., Jr., Two-stream plasma instability as a source of irregularities in the ionosphere, Phys. Rev. Letters, 10, 279 - 282, 1963.

Fejer, J. A. and W. Calvert, Resonance effects of electrostatic oscillations in the ionosphere, J. Geophys. Res., 69, 5049 - 5062, 1964.

Fredricks, R. W., Production of superthermal electrons by electrostatic plasma oscillations, submitted to Phys. Fluids, 1965.

Fredricks, R. W., F. L. Scarf, and W. Bernstein, Numerical estimates of superthermal electron production by ion acoustic waves in the transition region, J. Geophys. Res., 70, 21 - 28, 1965.

Fritz, T. A. and D. A. Gurnett, Diurnal and latitudinal effects observed for 10-kev electrons at low satellite orbits, J. Geophys. Res., 70, 2485 - 2502, 1965.

Gurnett, D. A. and B. J. O'Brien, High-latitude geophysical studies with satellite Injun 3, 5, Very low frequency electromagnetic radiation, J. Geophys. Res., 69, 65 - 89, 1964.

Hall, D. F., R. F. Kemp, and J. M. Sellen, Jr., Plasma-vehicle interaction in a plasma stream, AIAA Journal, 2, 1032 - 1039, 1964.

Harris, E. G. Plasma instabilities associated with anisotropic velocity distributions, J. Nucl. Energy, Pt. C, 2, 138 - 145, 1961.

Hilton, H. H., J. R. Stevens, and A. L. Vampola, Observations of large fluxes of low-energy protons, Trans. A.G.U., 45, 602, 1964.

Huguenin, G. R., A. E. Lilley, W. H. McDonough, and M. D. Papagiannis, Measurements of radio noise at 0.7 Mc and 2.200 Mc from a high-altitude rocket probe, Planetary and Sp. Science, 12, 1157 - 1167, 1964.

LaQuey, R. E., B. J. O'Brien, and L. Westerlund, Millisecond resolution measurements of nearly monoenergetic auroral electrons, Trans. A.G.U., 46, 529, 1965.

Liemohn, H. B. and F. L. Scarf, Whistler determination of electron energy and density distributions in the magnetosphere, J. Geophys. Res., 69, 883 - 904, 1964.

McDiarmid, I. B. and J. R. Burrows, Electron fluxes at 1000 kilometers associated with the tail of the magnetosphere, J. Geophys. Res., 70, 3031 - 3044, 1965.

O'Brien, B. J., High-latitude geophysical studies with satellite Injun 3, 3, Precipitation of electrons into the atmosphere, J. Geophys. Res., 69, 13 - 44, 1964.

Perkins, F. W., E. E. Salpeter, and K. O. Yngvesson, Incoherent scatter from plasma oscillations in the ionosphere, Phys. Rev. Letters, 14, 579 - 581, 1965.

Rosenbluth, M. N. and R. F. Post, High-frequency electrostatic plasma instability inherent to "loss-cone" particle distributions, Phys. Fluids, 8, 547 - 550, 1965.

Rostoker, N., Fluctuations of plasmas, 1, Nucl. Fusion, 1, 101 - 120, 1961.

Samir, U. and A. P. Willmore, The distribution of charged particles near a moving spacecraft, Plan. and Sp. Sci., 13, 285 - 296, 1965.

Scarf, F. L., G. M. Crook, and R. W. Fredricks, Preliminary report on the detection of electrostatic ion waves in the magnetosphere, J. Geophys. Res., 70, 3045 - 3060, 1965.

Scarf, F. L. and R. W. Fredricks, Direct detection of ambient electron plasma oscillation fields in the magnetosphere, Plan. and Sp. Sci., (in press) 1965.

Serbu, G. A., Results from the IMP-1 retarding potential analyzer, NASA Rept. X-615-64-109, Goddard Space Flight Center, Greenbelt, Maryland, May, 1964.

Sharp, R. D., J. B. Reagan, S. R. Salisbury, and L. F. Smith, Direct measurement of auroral electrons at low energies, J. Geophys. Res., 70, 2119 - 2128, 1965.

Smith, et al., An ion gyrofrequency phenomenon observed in satellites, Nature, 204, 274, 1964.

Sturrock, P. A., Dipole resonances in a homogeneous plasma in a magnetic field, Phys. Fluids, 8, 88 - 96, 1965.

Swift, D. W., A mechanism for energizing electrons in the magnetosphere, J. Geophys. Res., 70, 3061 -3074, 1965.

Swift, D. W., An interpretation of auroral breakup, University of Alaska Report NSF G-25193, July, 1965.

Westerlund, L., B. J. O'Brien, and R. E. Laquey, Coordinated study of an aurora with ground-based and rocket-borne instrumentation, Trans. A.G.U., 46, 528, 1965.

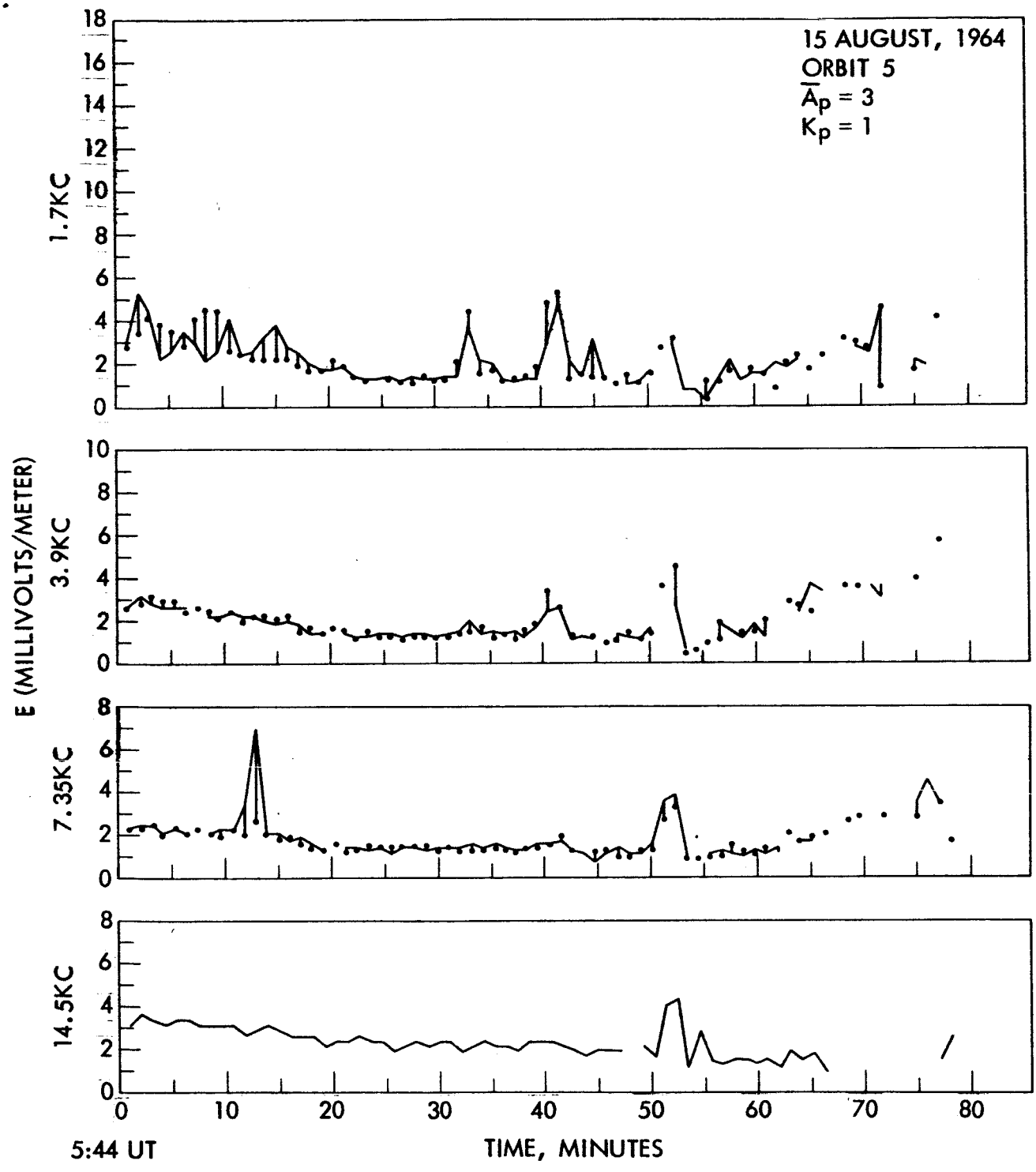

Figure 1. VLF electric fields measured on orbit 5. The continuous lines connect samples measured once every 1.068 minutes. On the three lowest frequency channels the vertical lines connect the first sample in each 1.068 minute sequence with a reading taken 7, 5, or 3 seconds later (f = 1.7, 3.9, 7.35 kc/s, respectively). Further comments about the data are contained in the text.

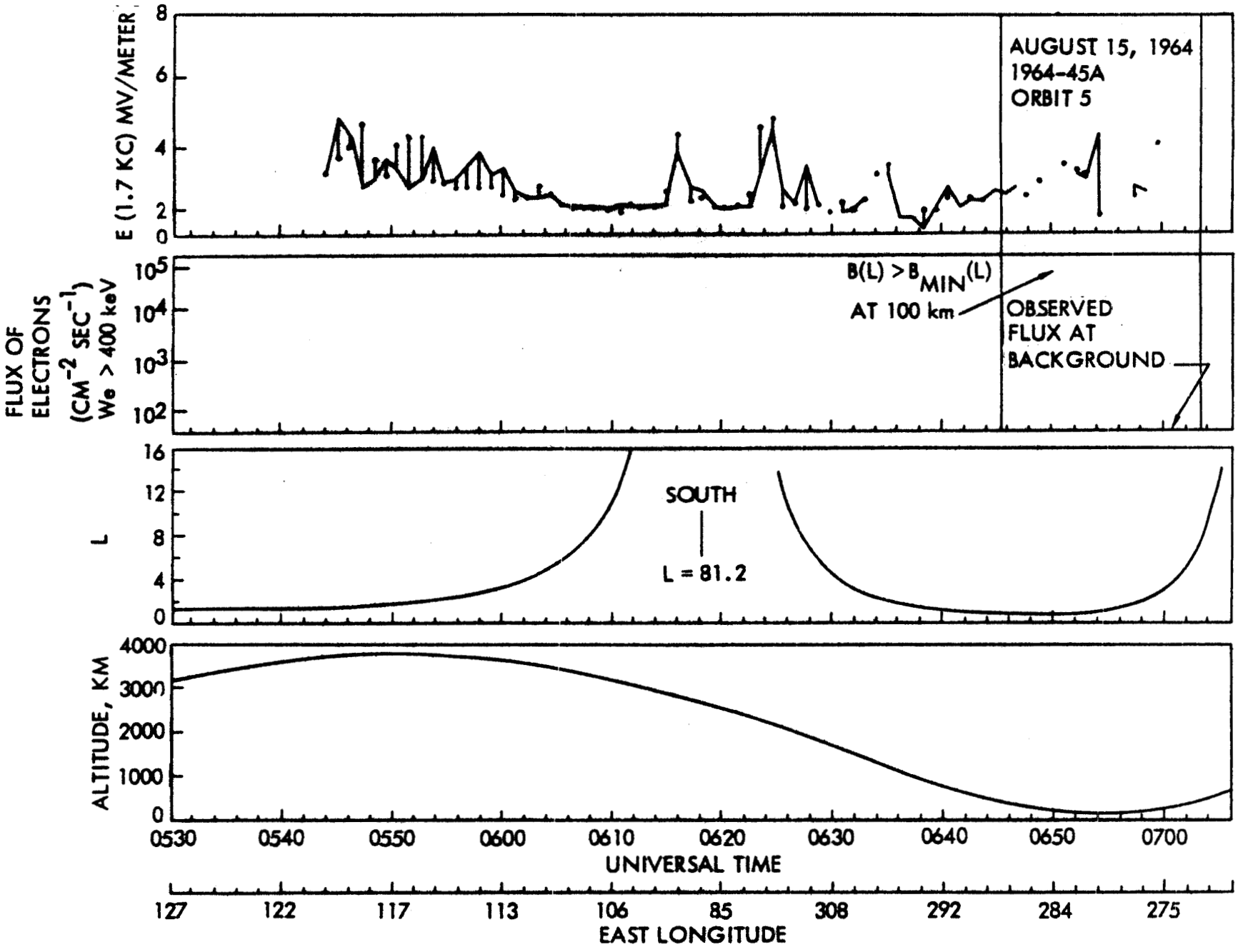

Figure 2. The 1.7 kc/s response for orbit 5, ephemeris parameters, and electron mode response of the Aerospace Corporation solid detector (courtesy of G. A. Paulikas, J. B. Blake, and S. C. Freden) in the region where B(L) > B_{min}(L) at 100 km (based on curves supplied by J. Vette). Further comments about the data are contained in the text.

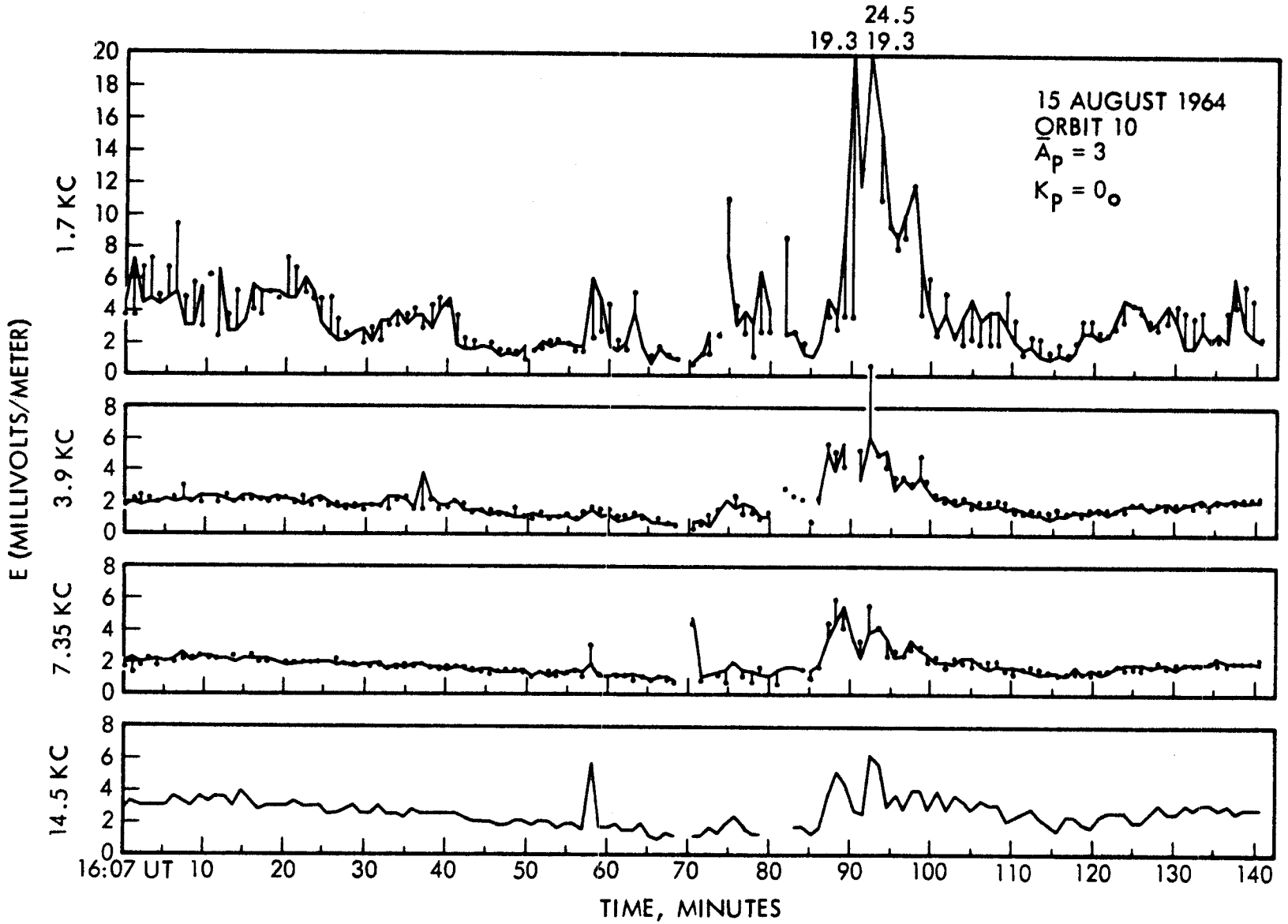

Figure 3. Data for orbit number 10 in same format as Figure 1.

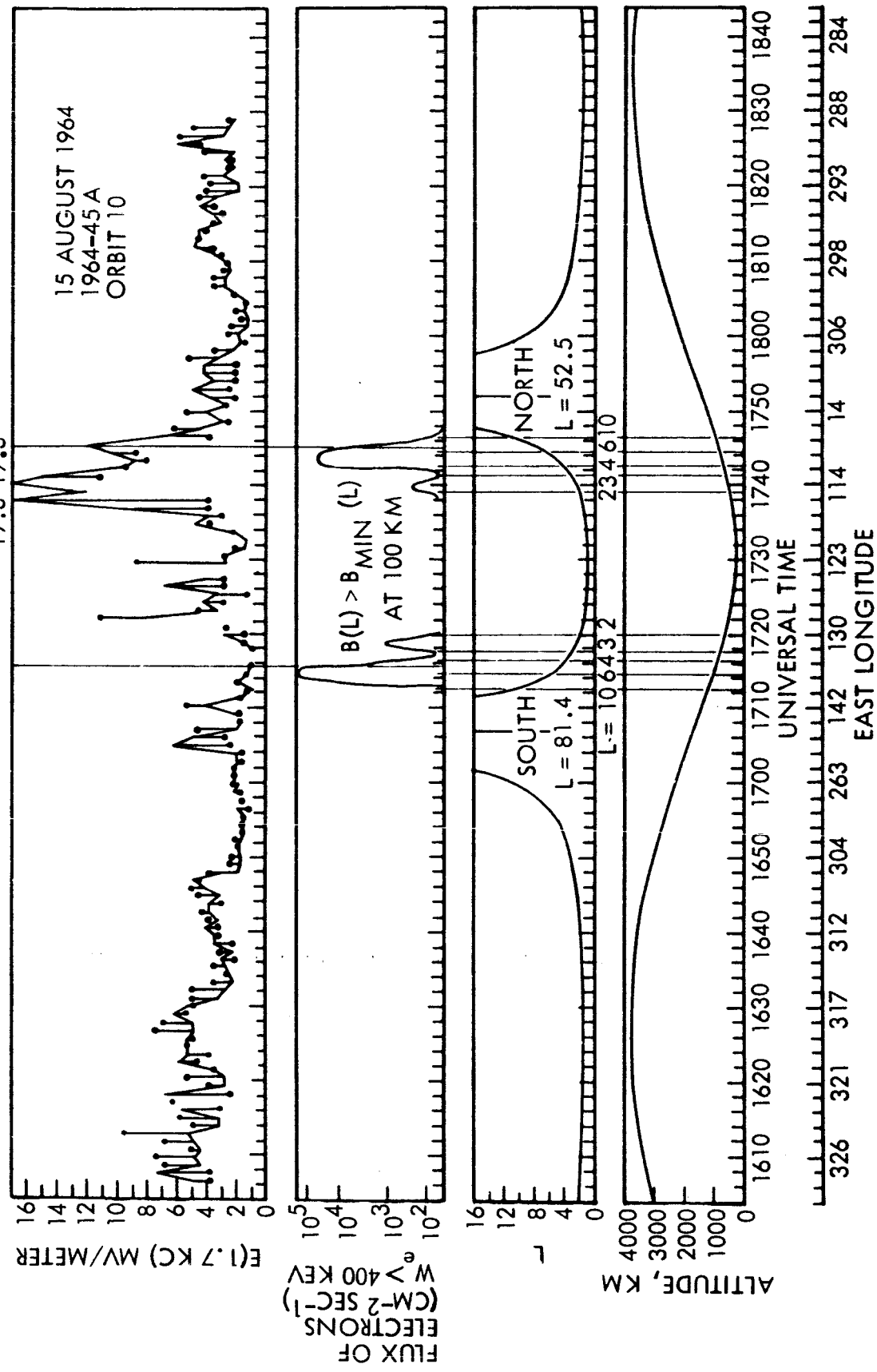

Figure 4. Data for orbit number 10 in same format as Figure 2.

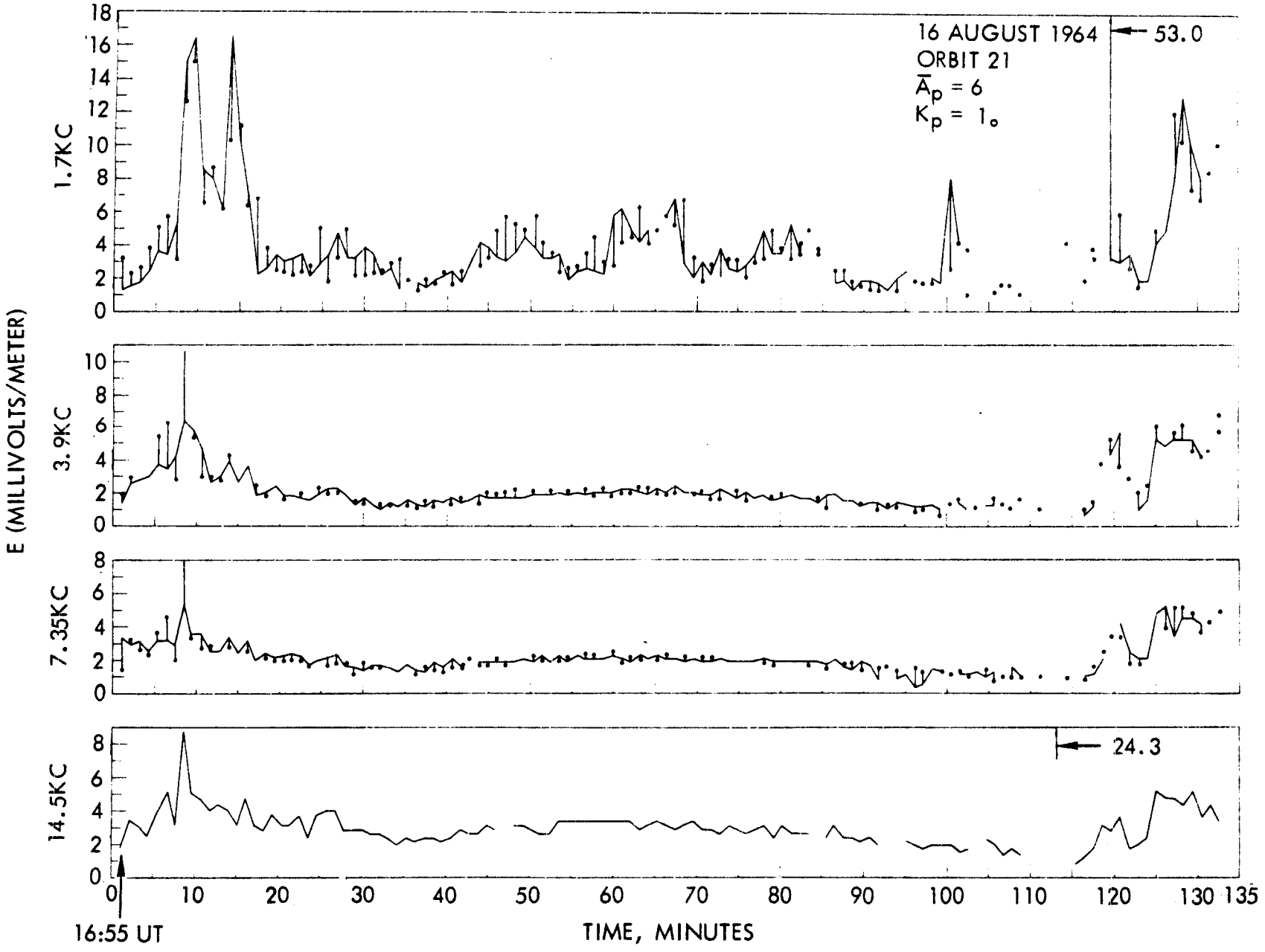

Figure 5. Data for orbit number 21 in same format as Figure 1.

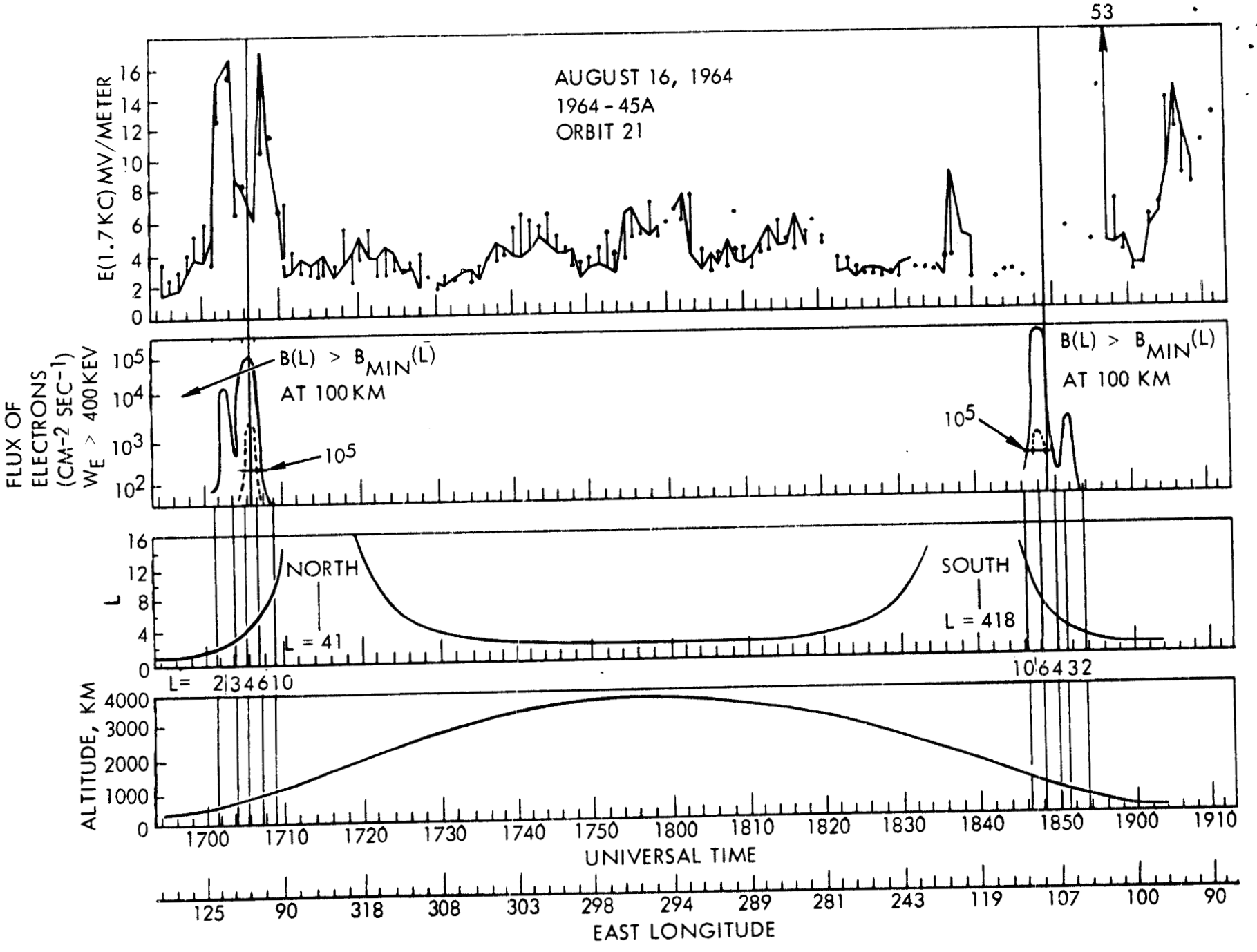

Figure 6. Data for orbit number 21 in same format as Figure 2.

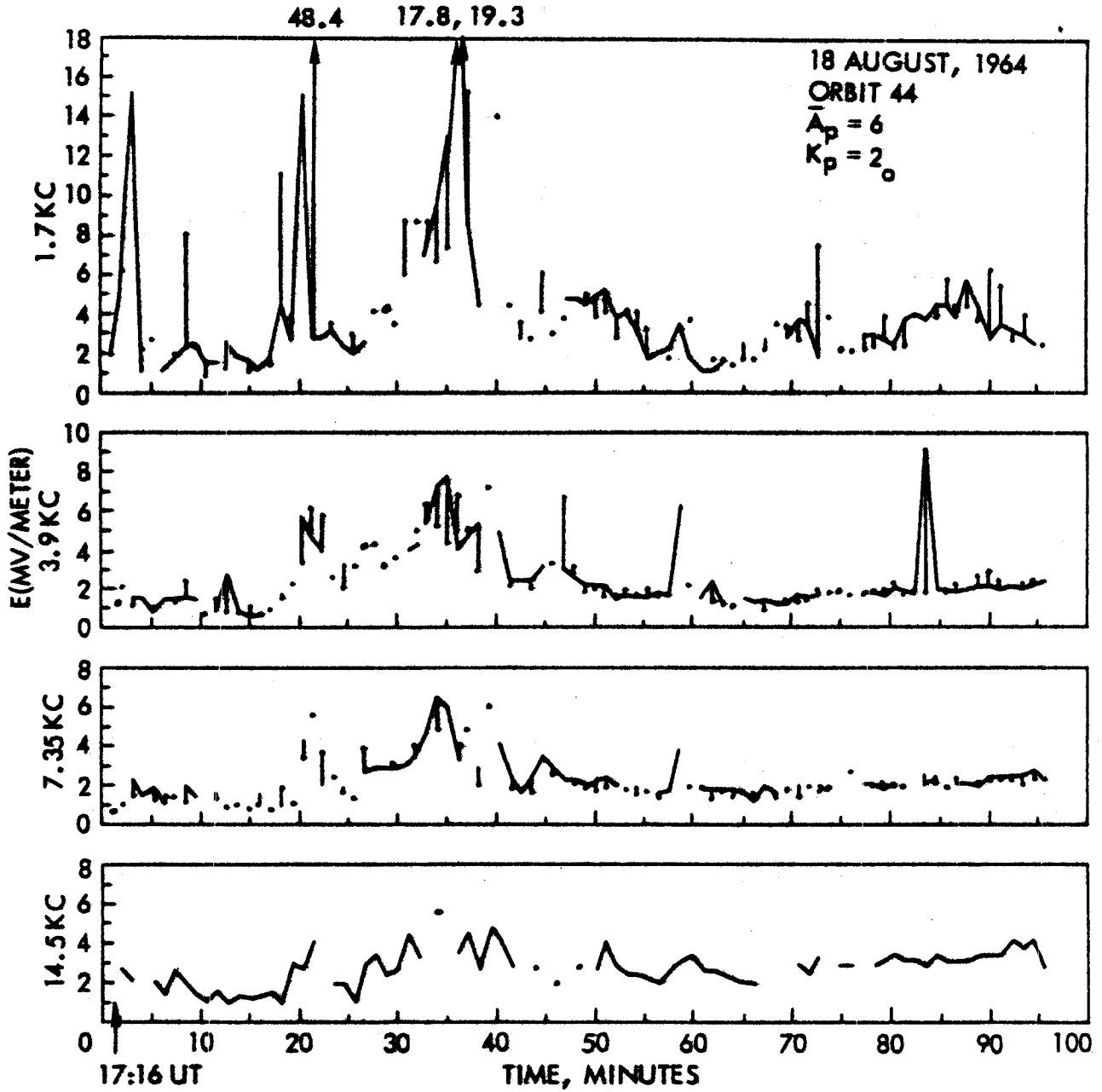

Figure 7. Data for orbit number 44 in same format as Figure 1.

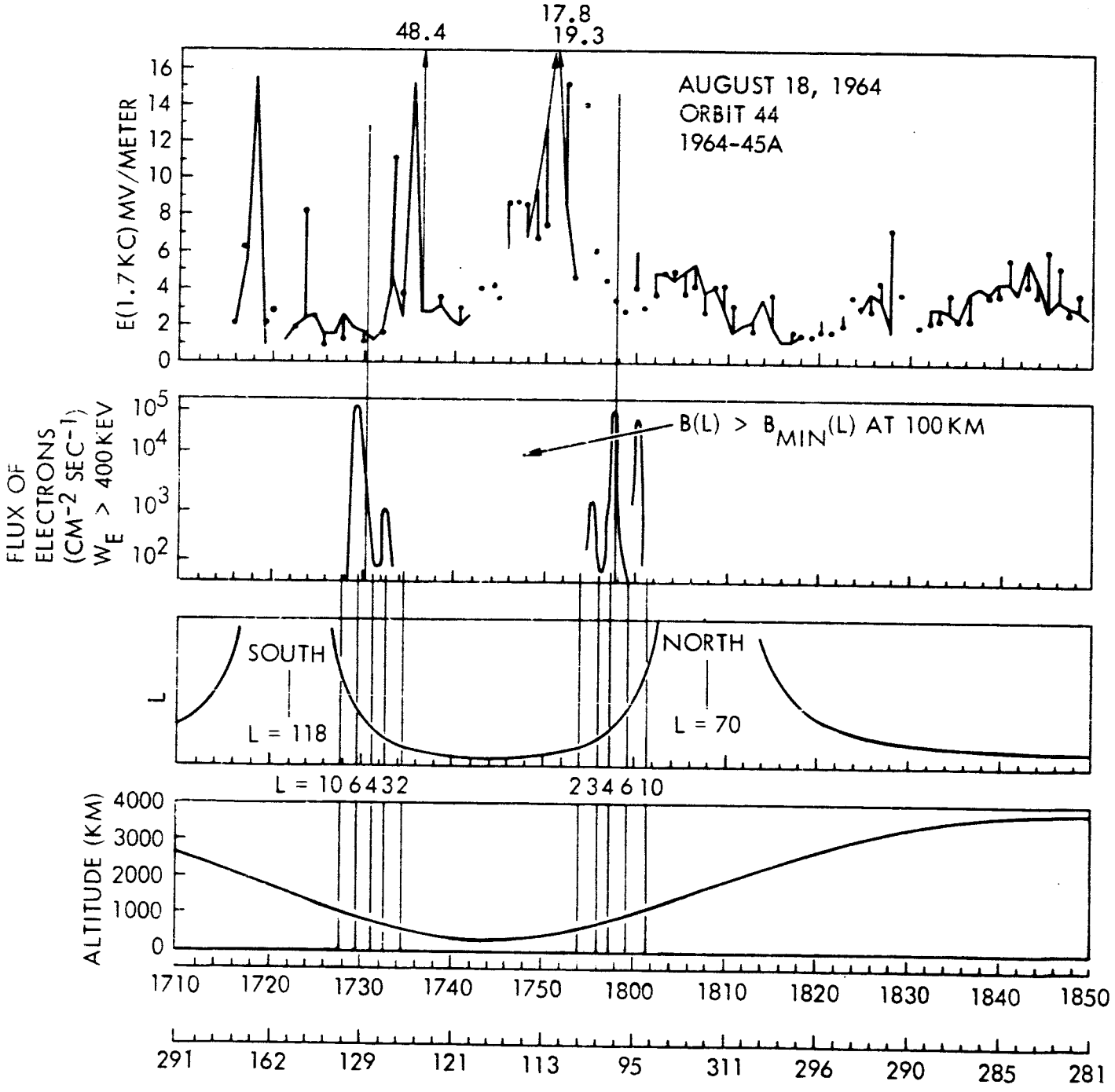

Figure 8. Data for orbit number 44 in same format as Figure 2.

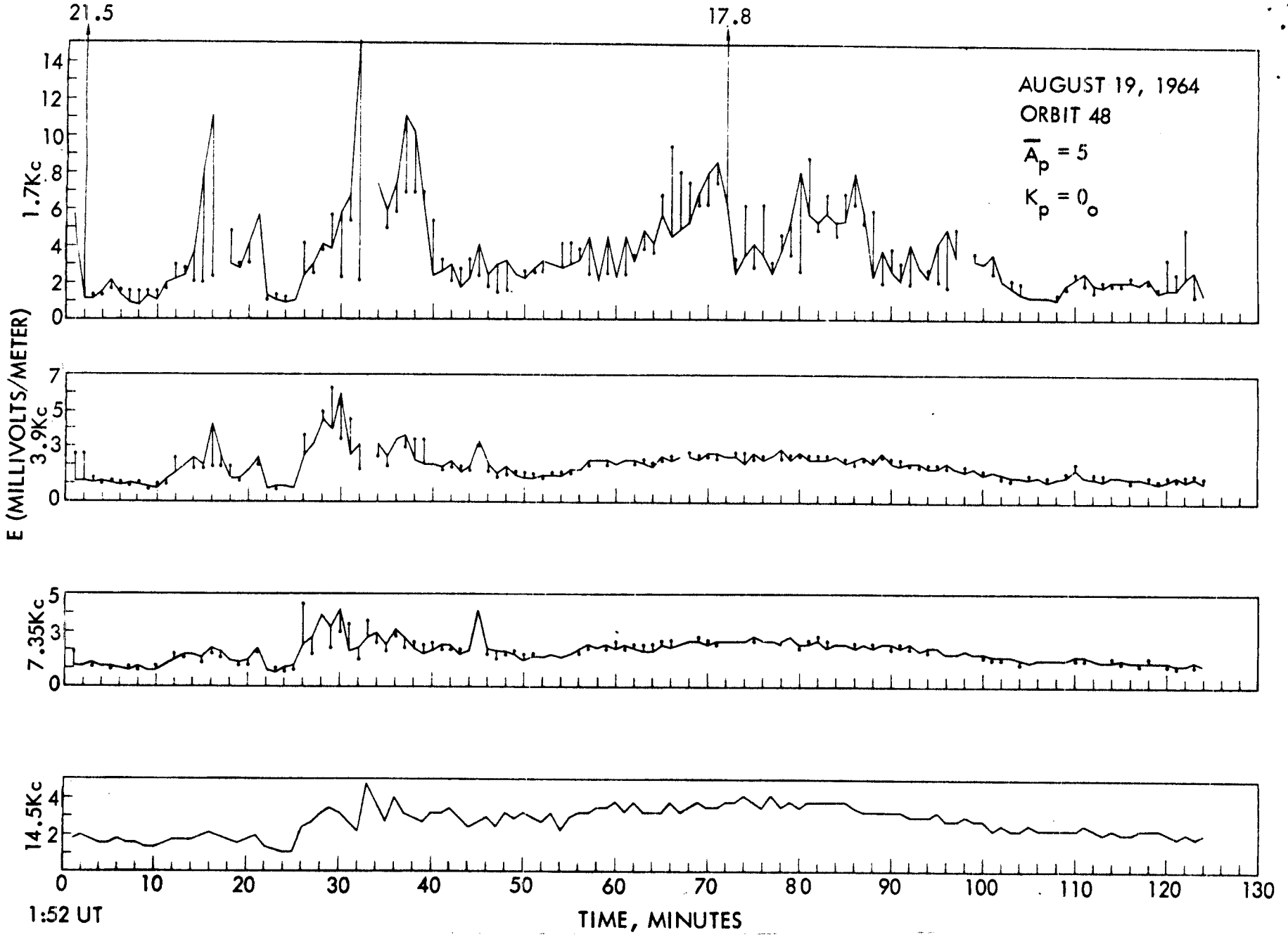

Figure 9. Data for orbit number 48 in same format as Figure 1

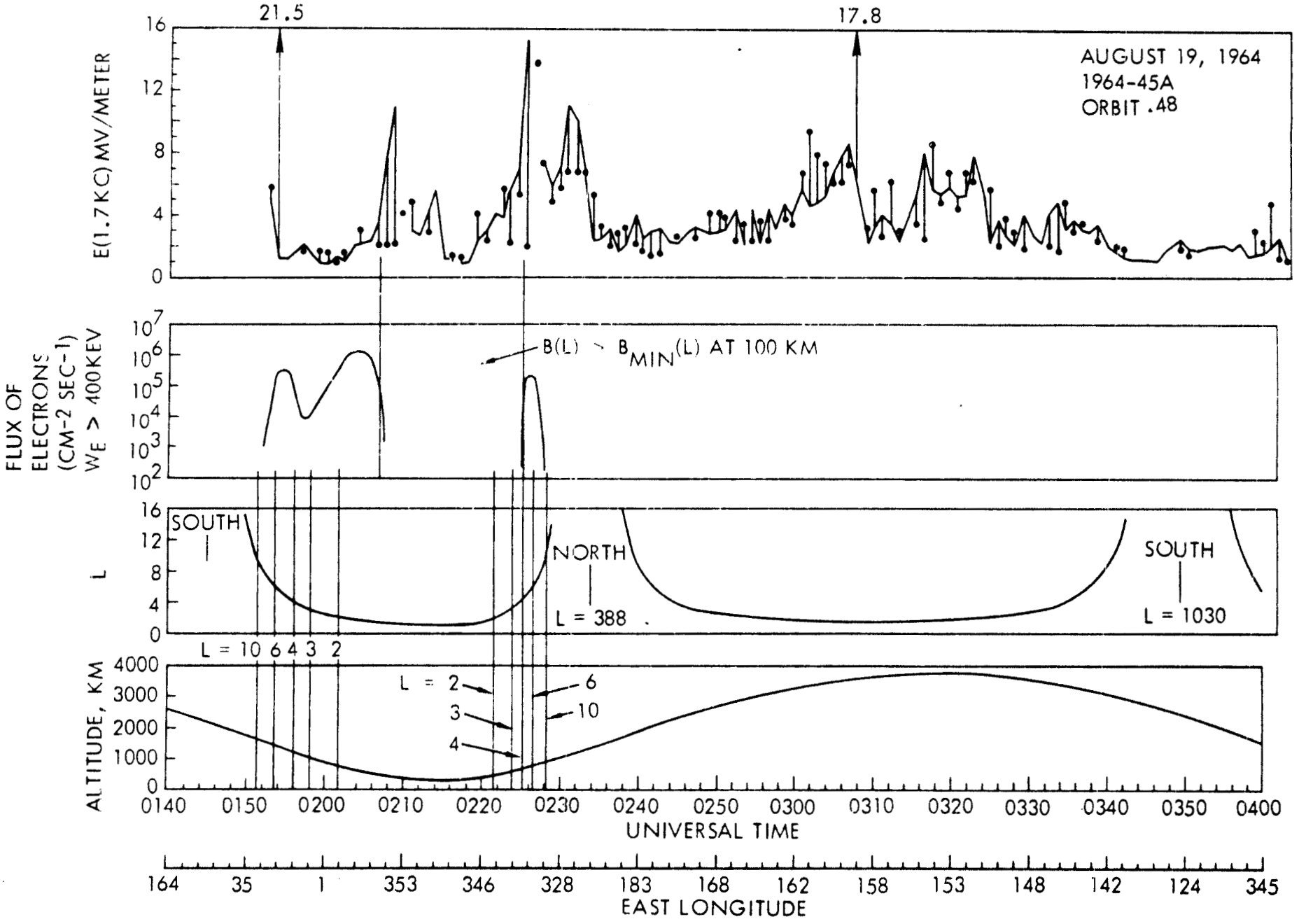

Figure 10. Data for orbit number 48 in same format as Figure 2.

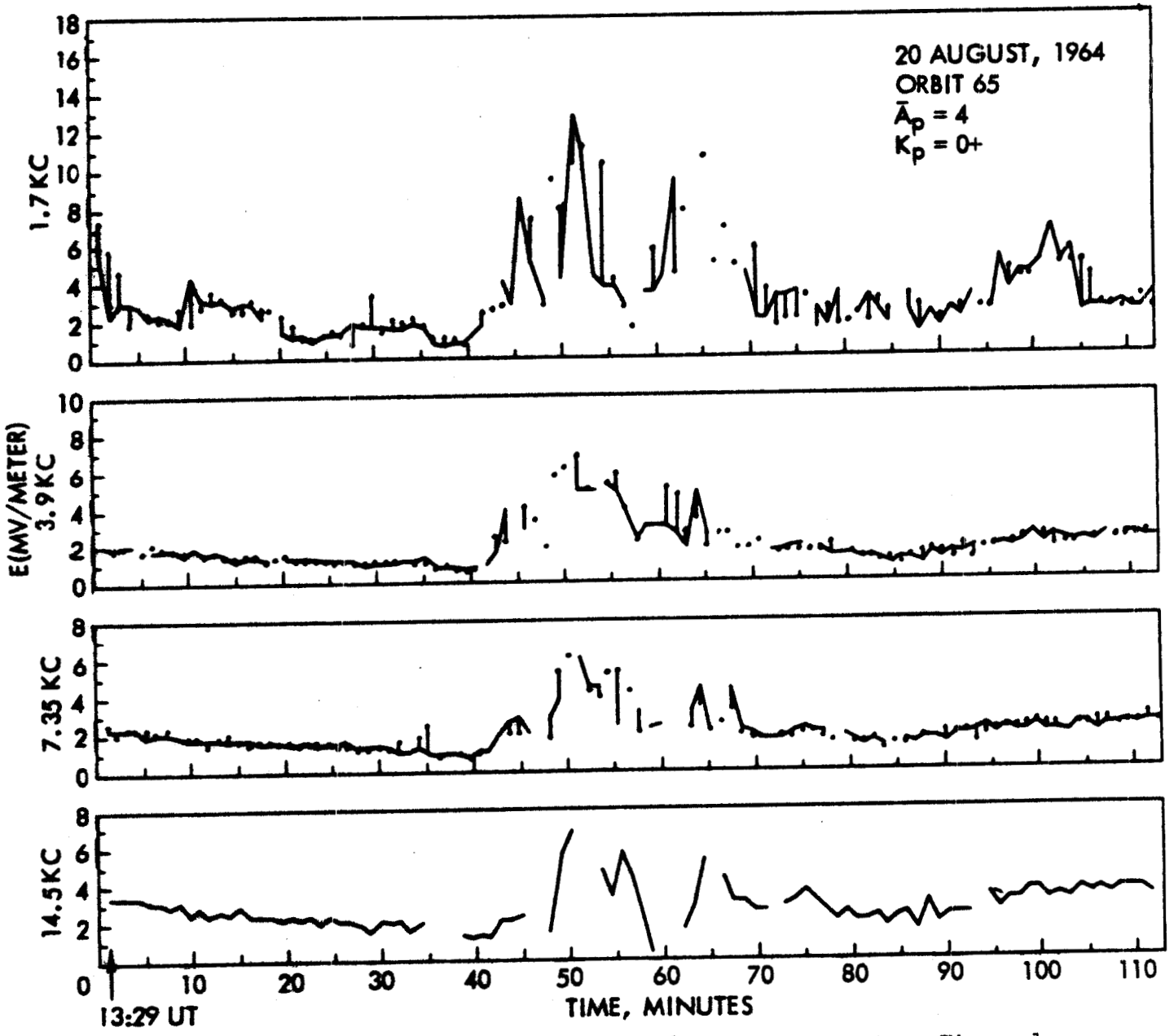

Figure 11. Data for orbit number 65 in same format as Figure 1.

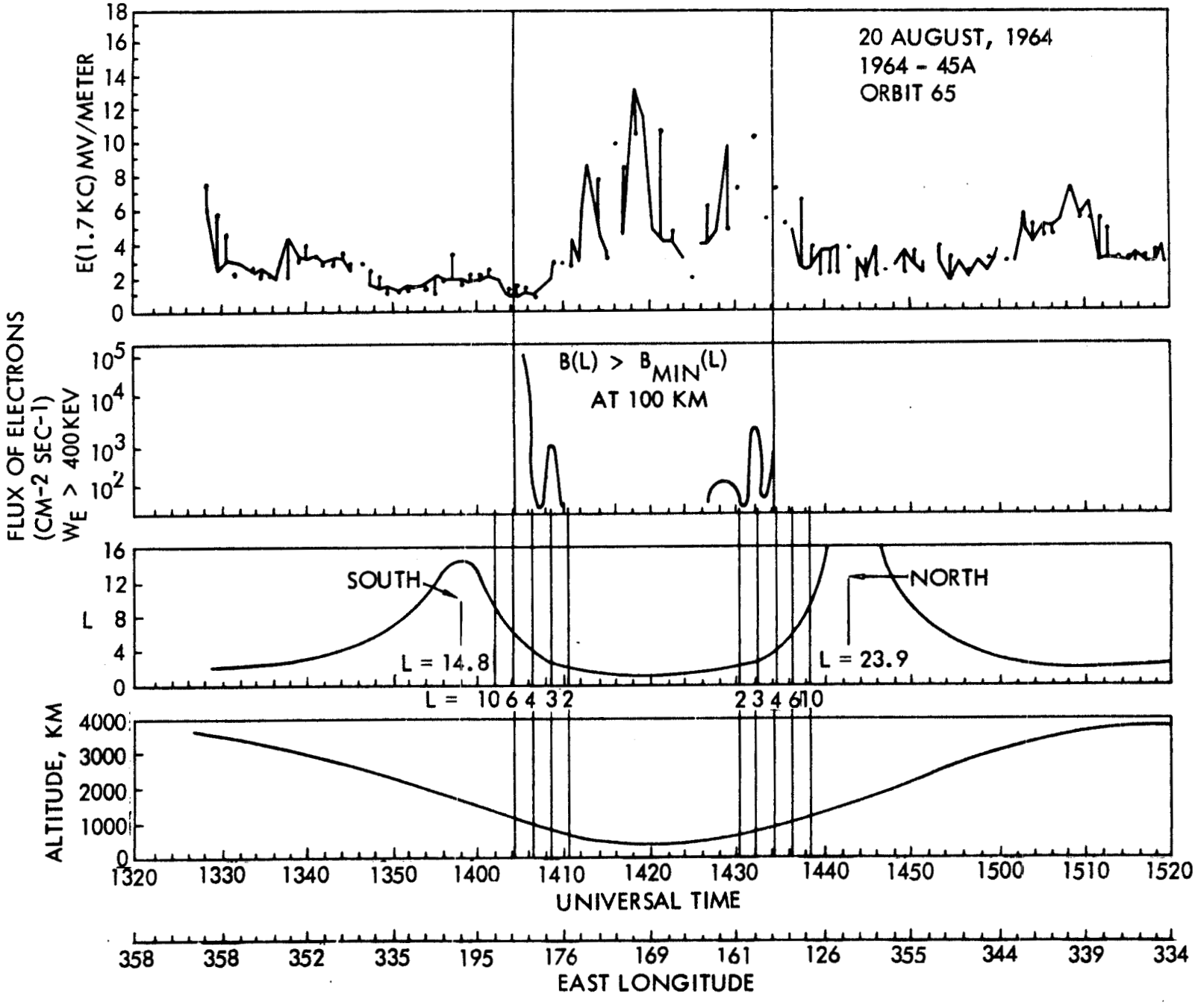

Figure 12. Data for orbit 65 in same format as Figure 2.

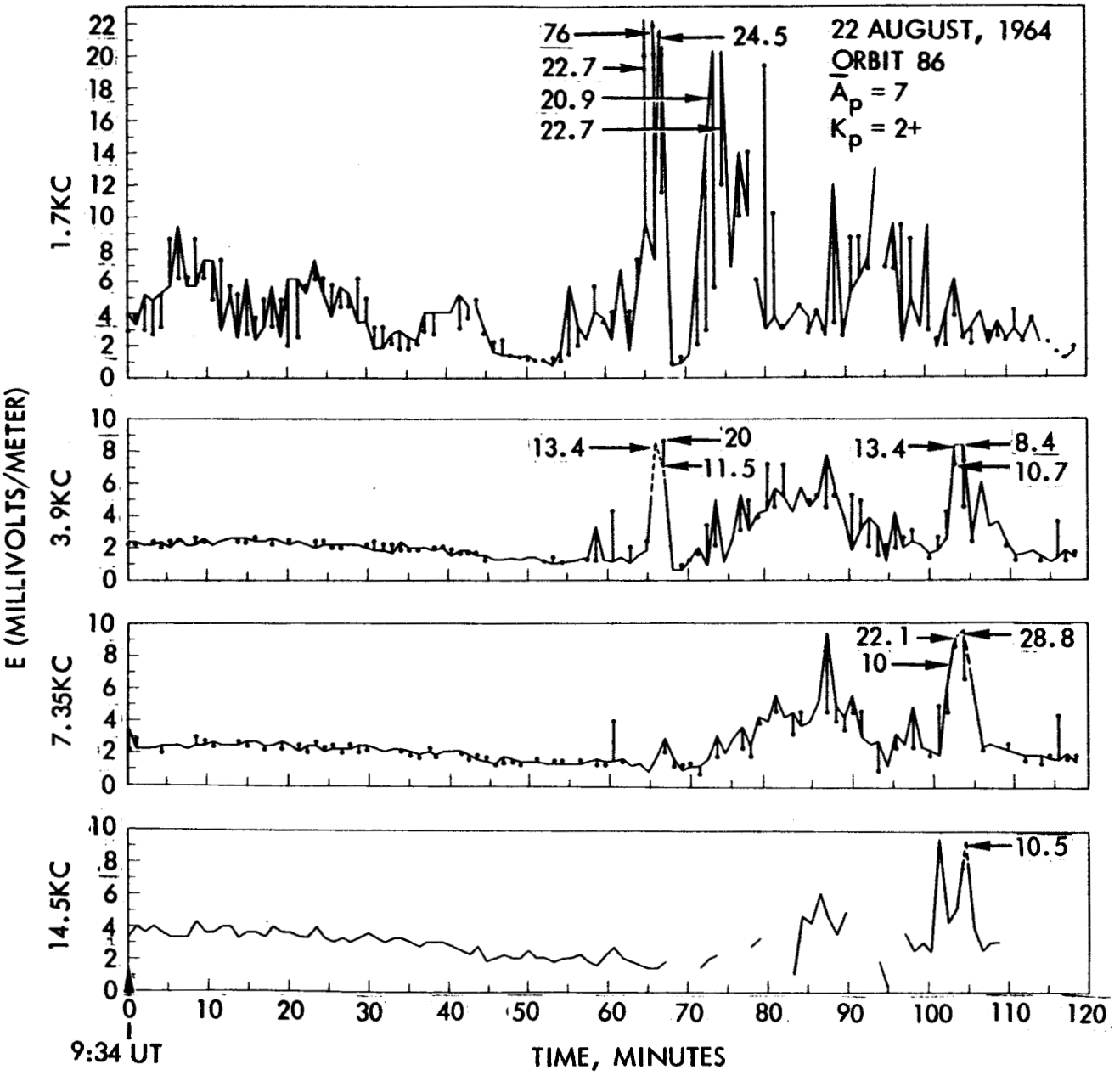

Figure 13. Data for orbit number 86 in same format as Figure 1.

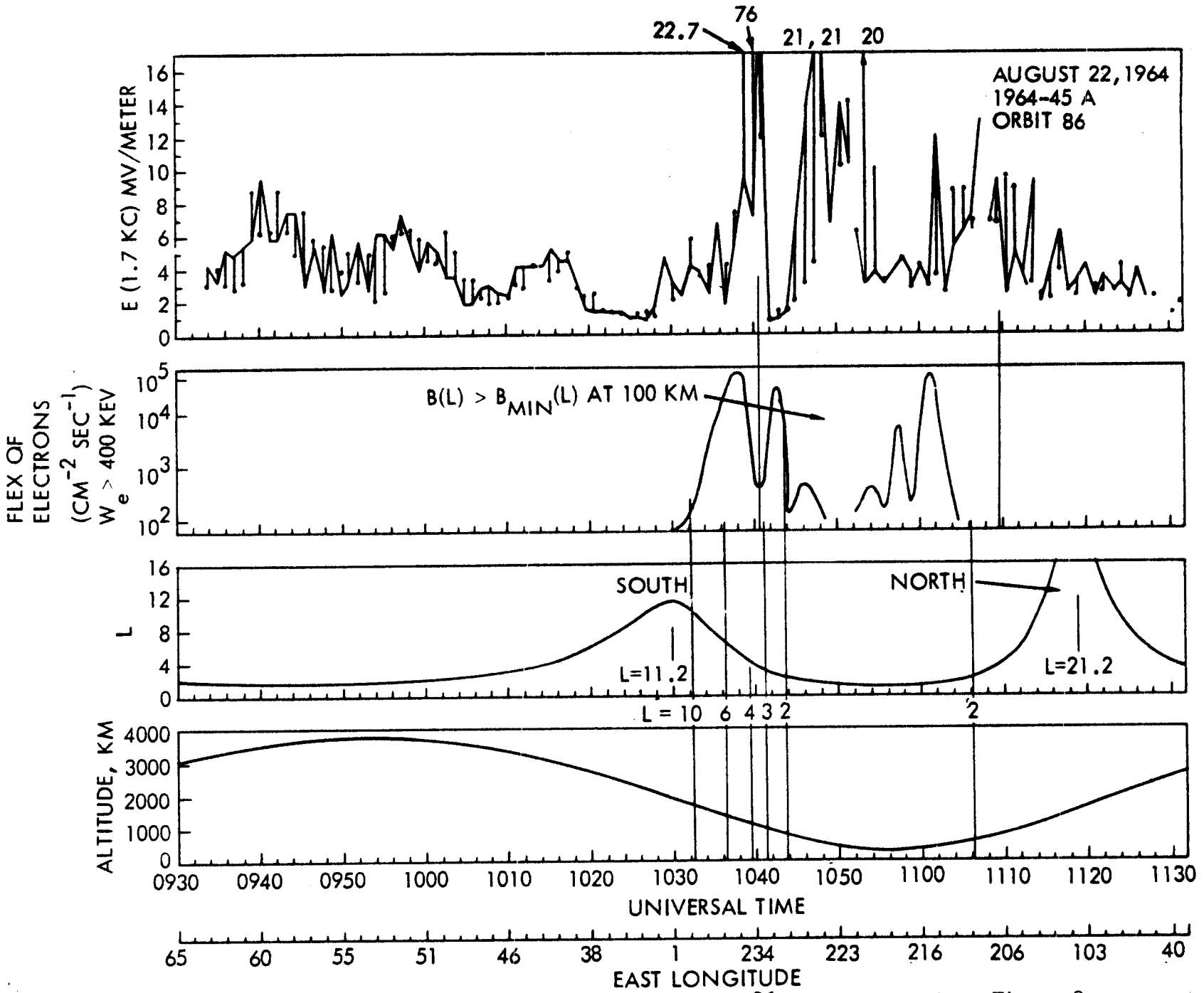

Figure 14. Data for orbit number 86 in same format as Figure 2.

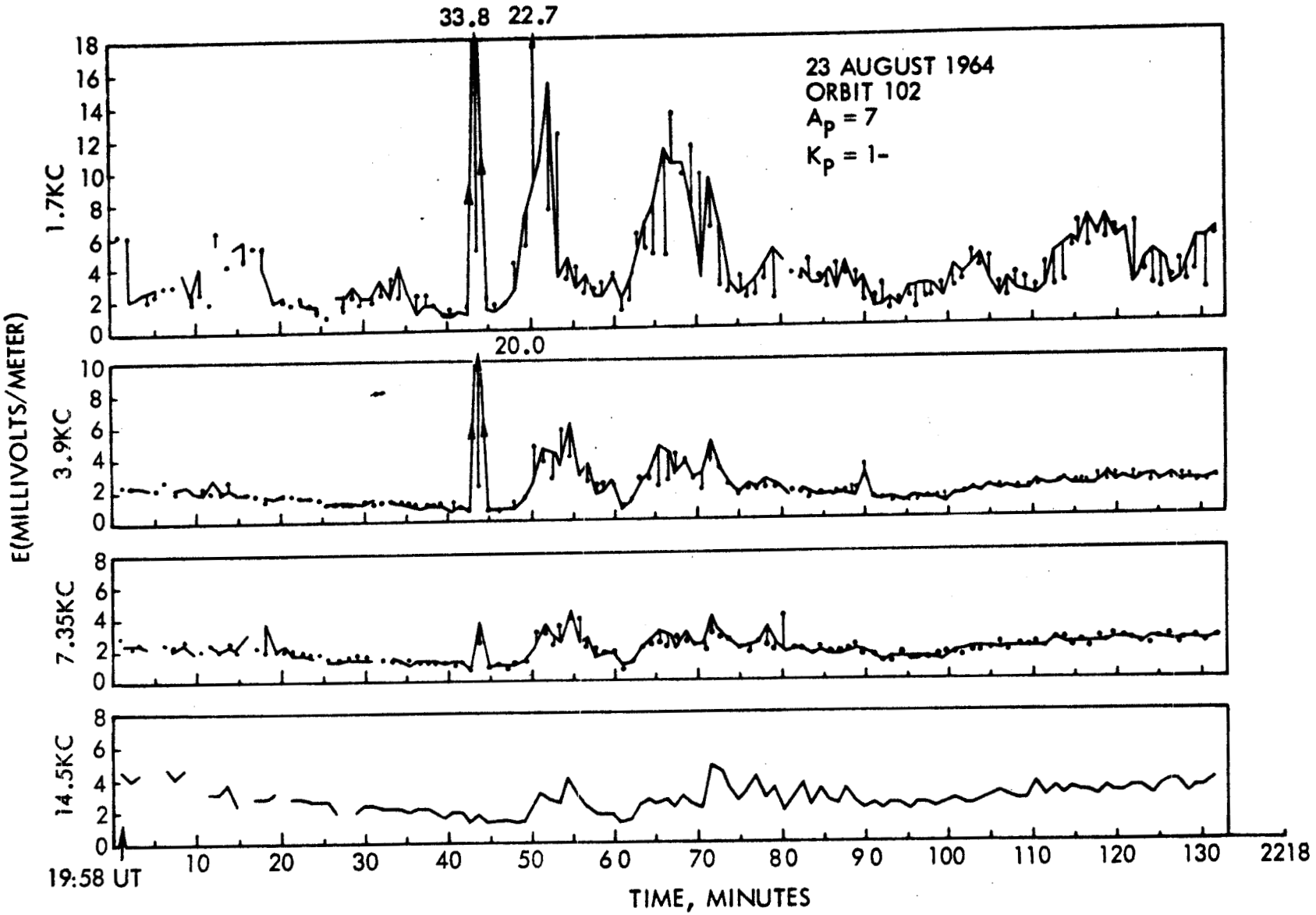

Figure 15. Data for orbit number 102 in same format as Figure 1.

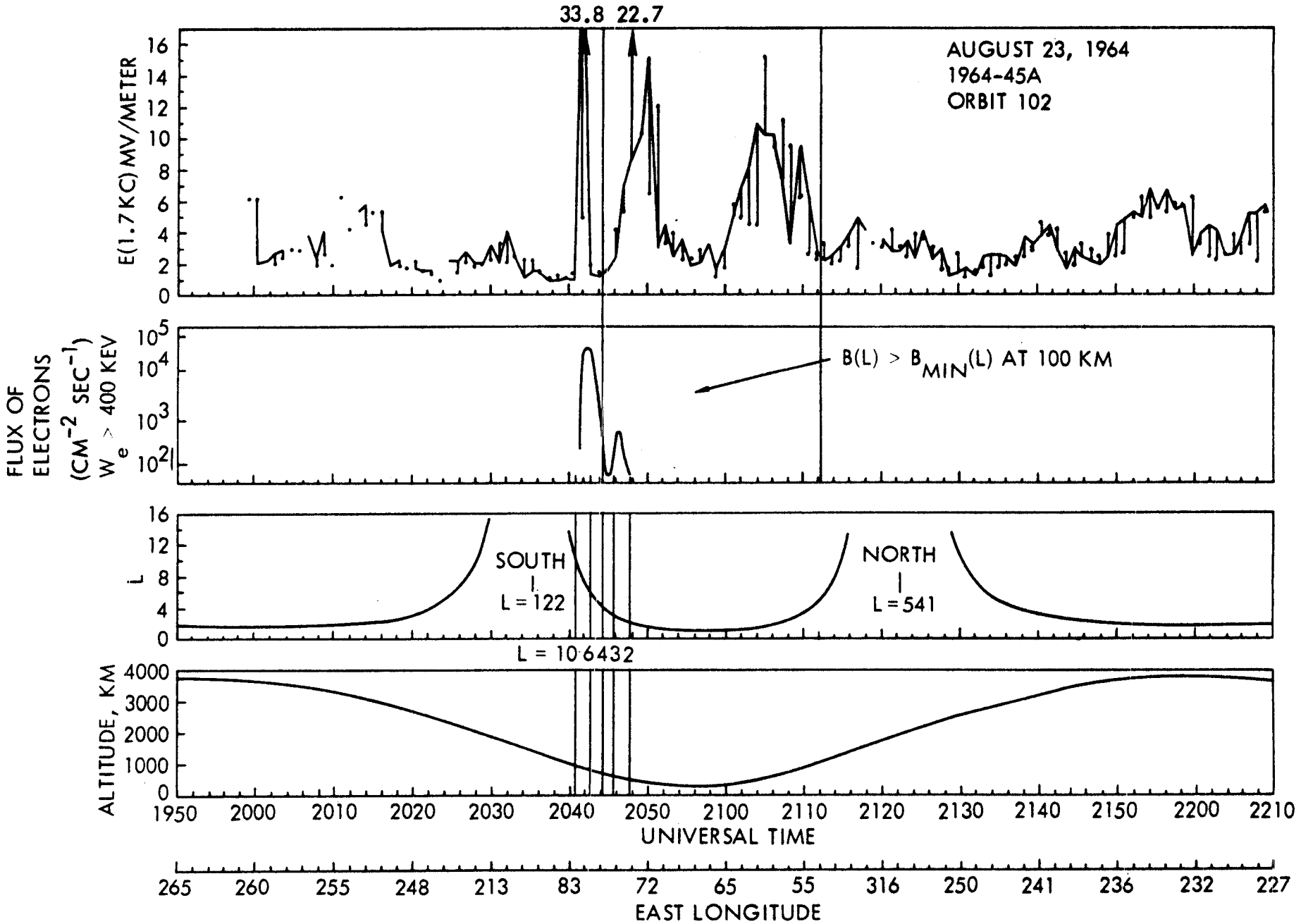

Figure 16. Data for orbit number 102 in same format as Figure 2.

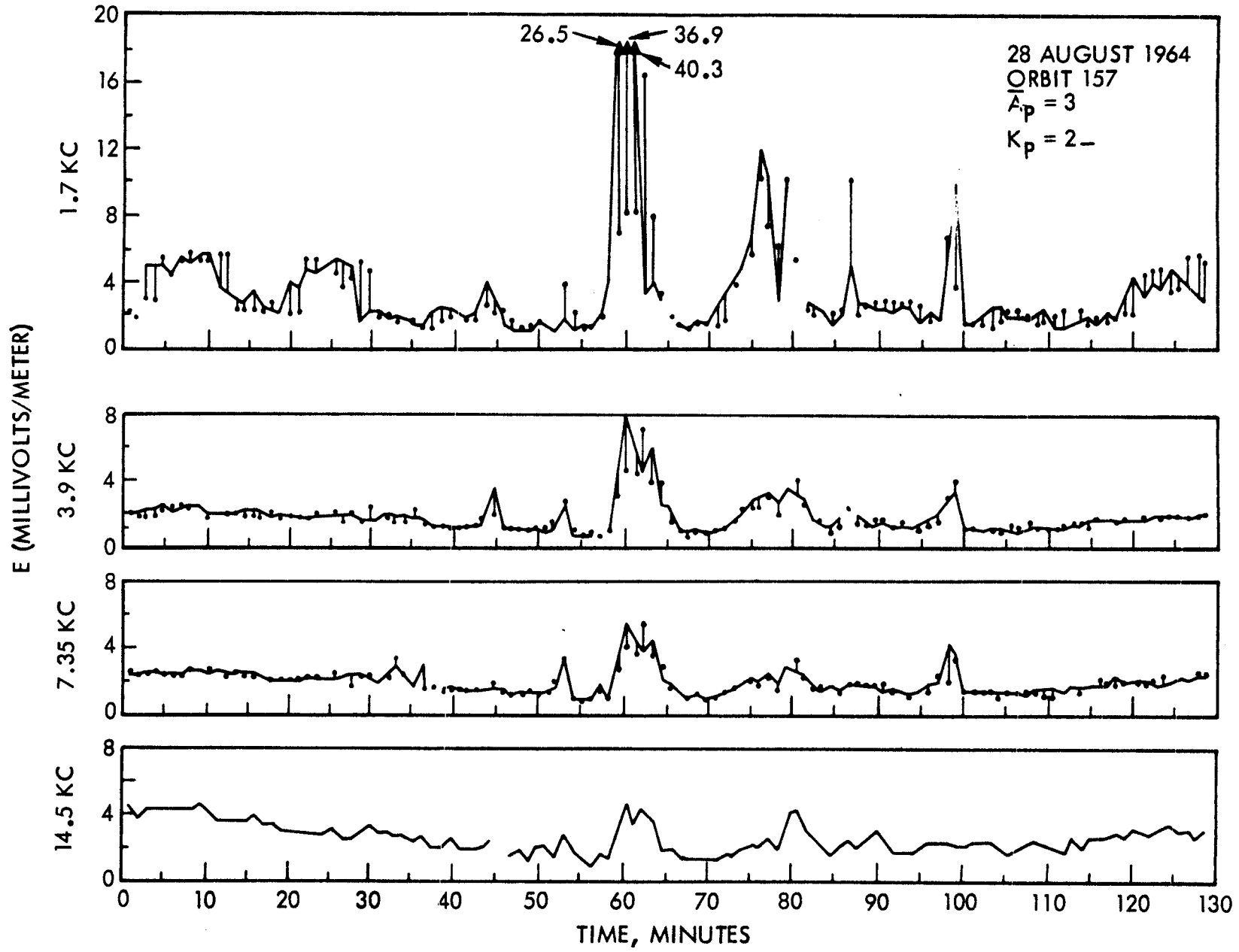

Figure 17. Data for orbit number 157 in same format as Figure 1.

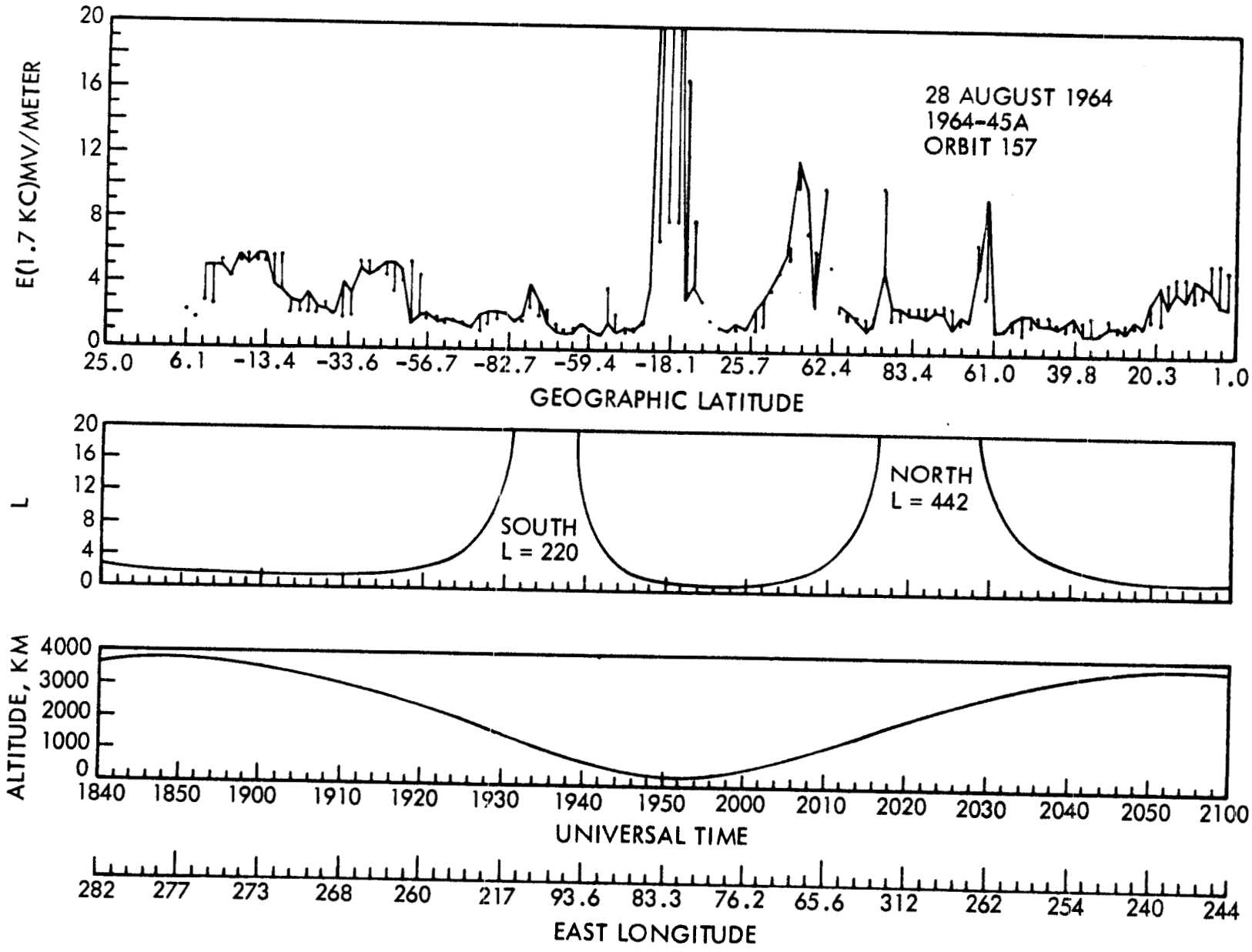

Figure 18. Data for orbit number 157 in same format as Figure 2 but no electron measurements are available.

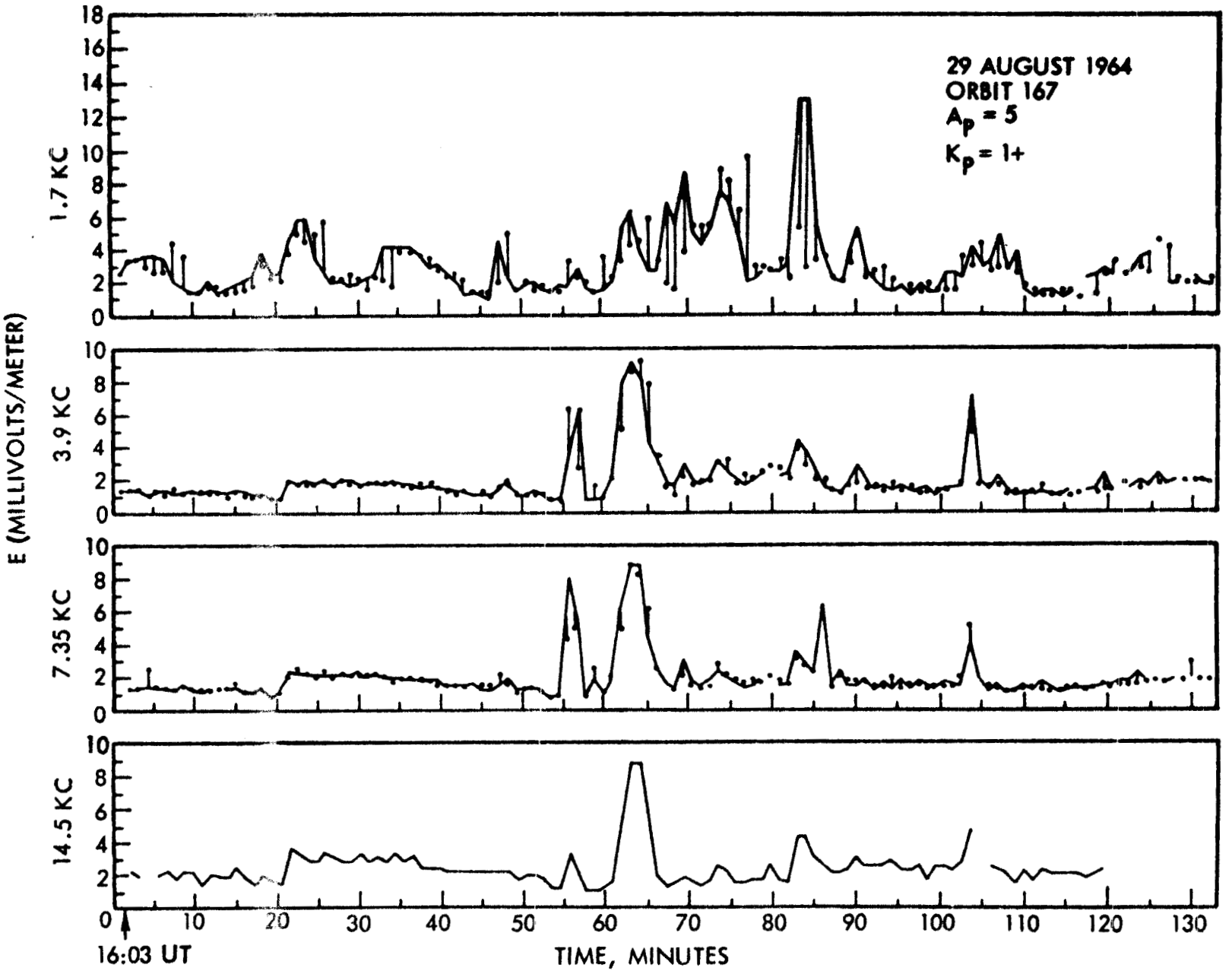

Figure 19. Data for orbit number 167 in same format as Figure 1.

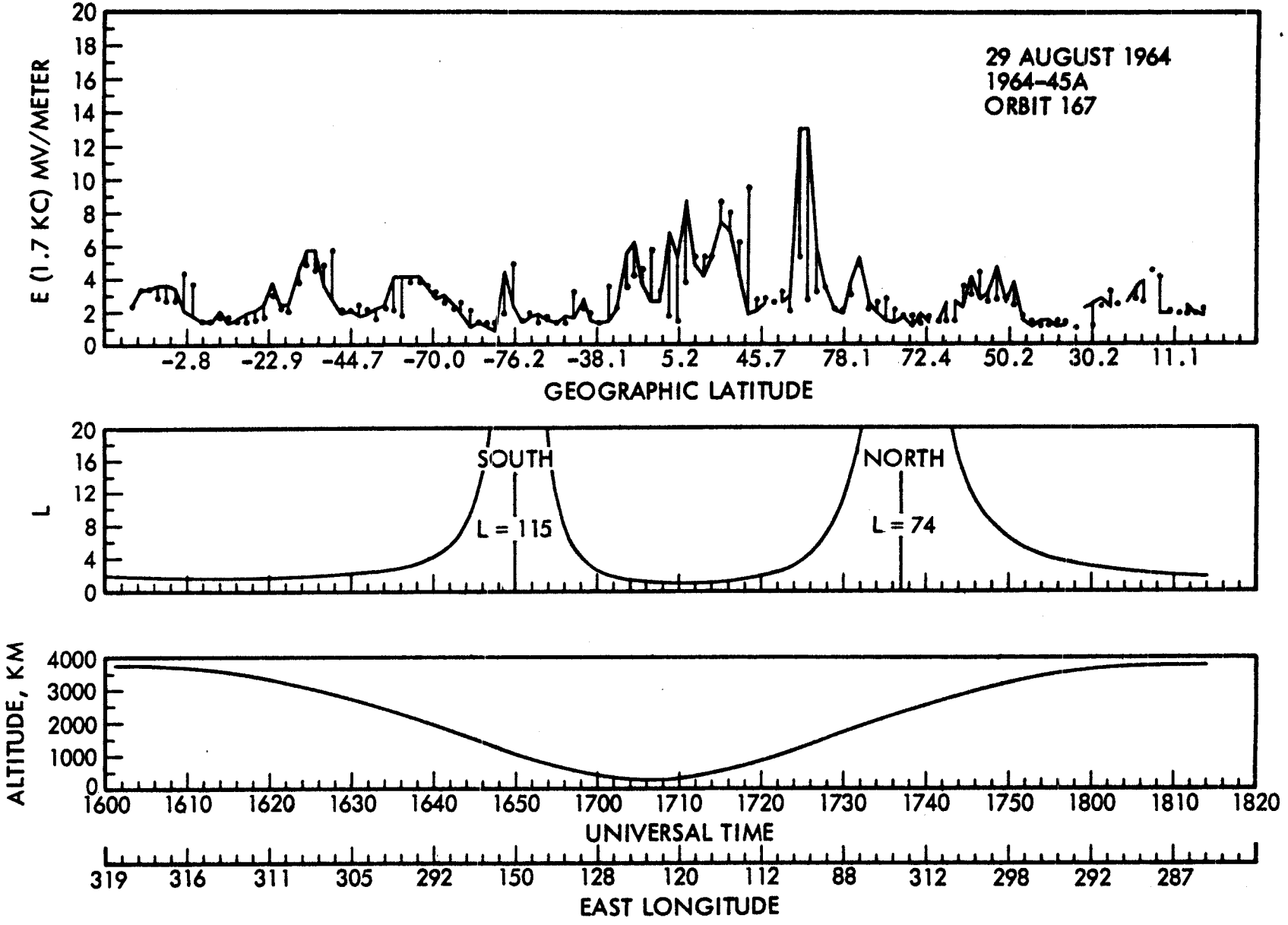

Figure 20. Data for orbit number 167 in same format as Figure 2 but no electron measurements are available.

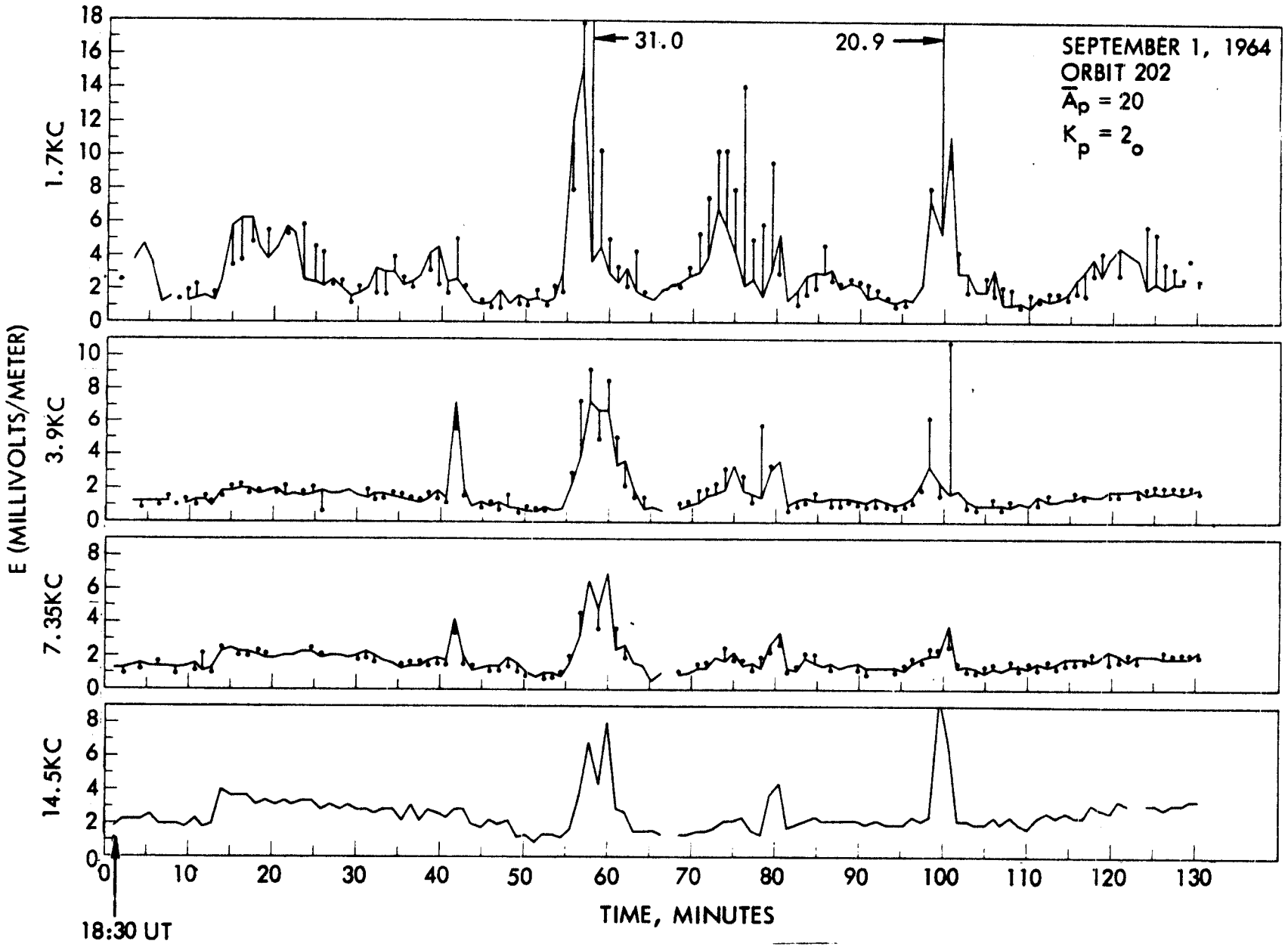

Figure 21. Data for orbit number 202 in same format as Figure 1

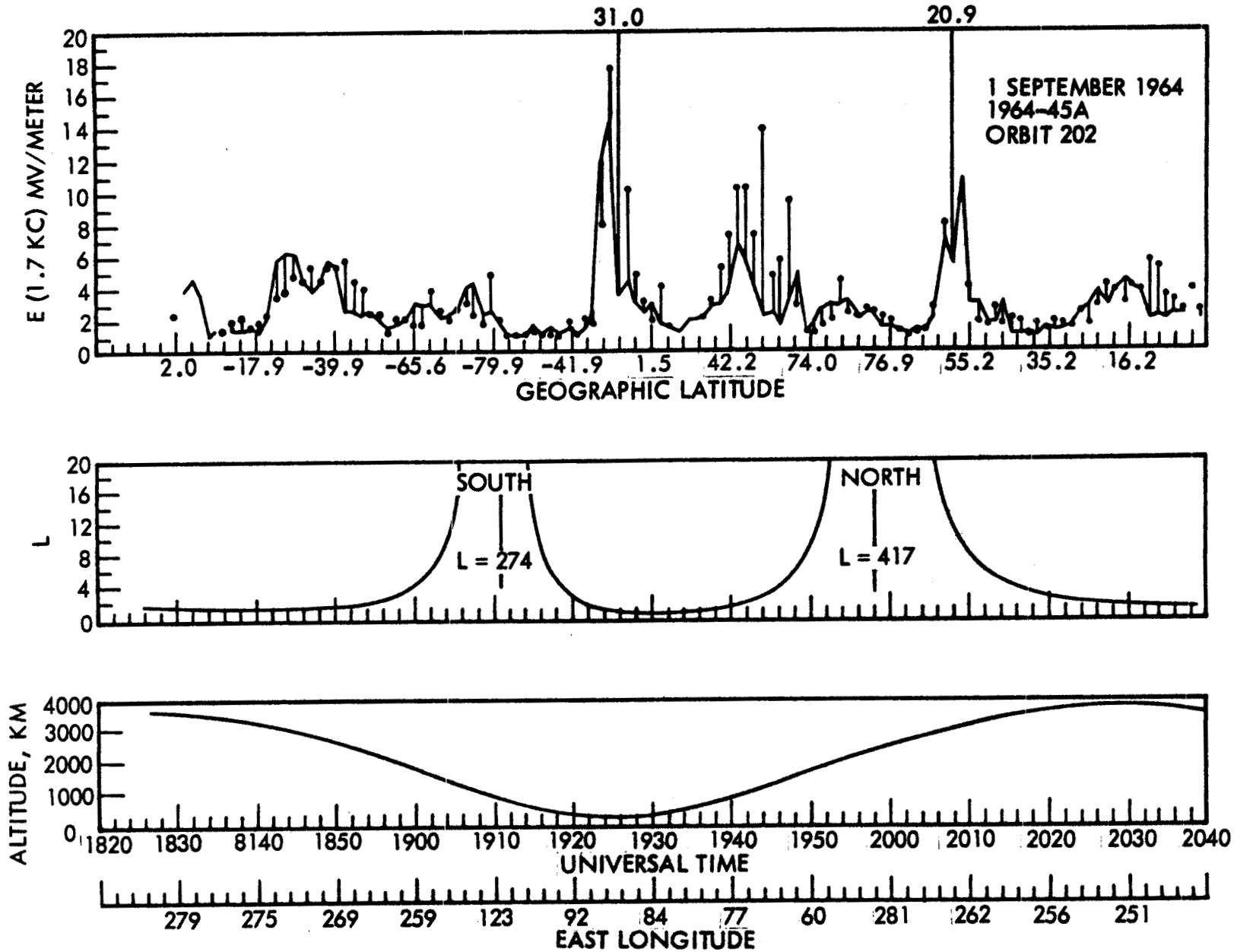

Figure 22. Data for orbit number 202 in same format as Figure 2 but no electron measurements are available.

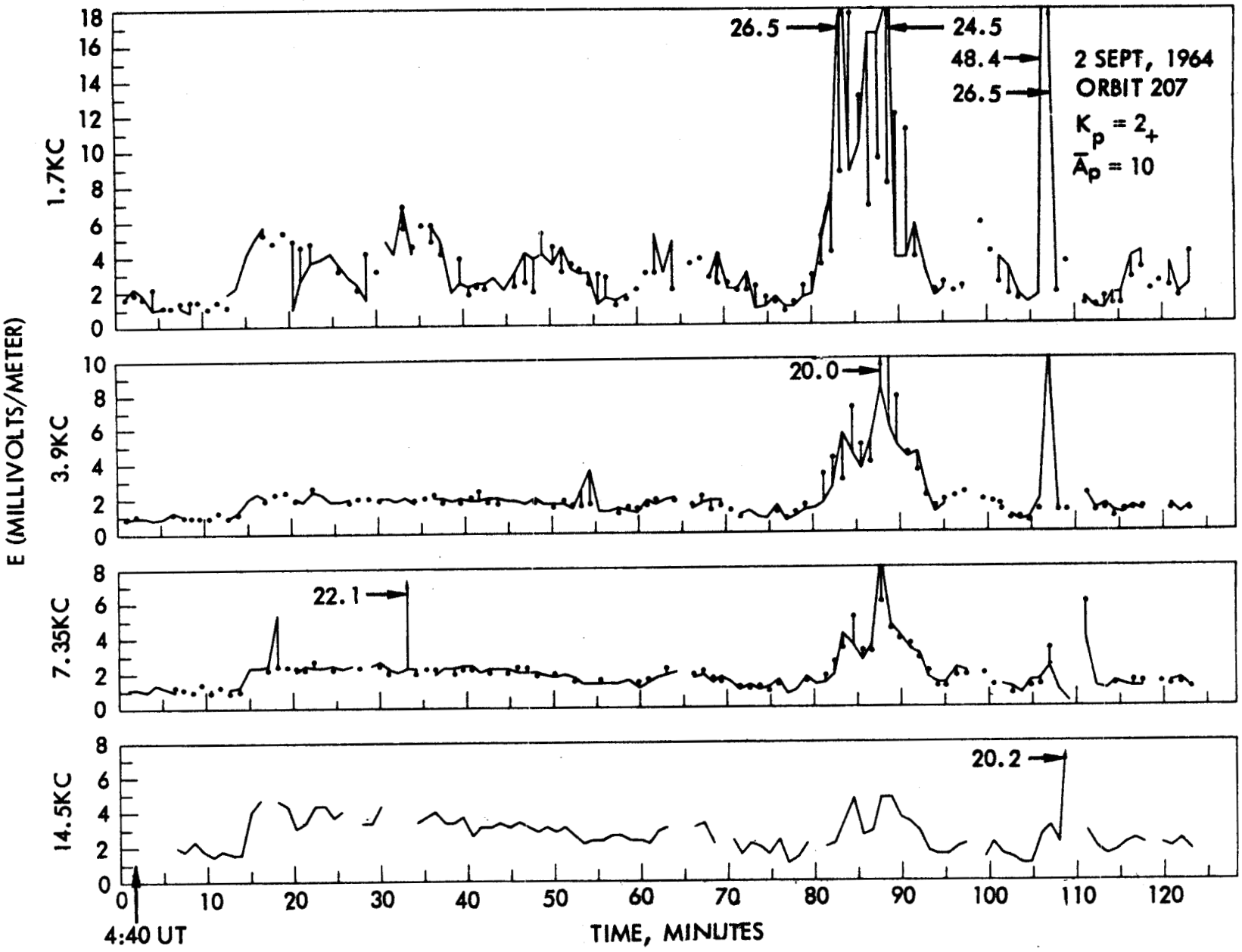

Figure 23. Data for orbit number 207 in same format as Figure 1.

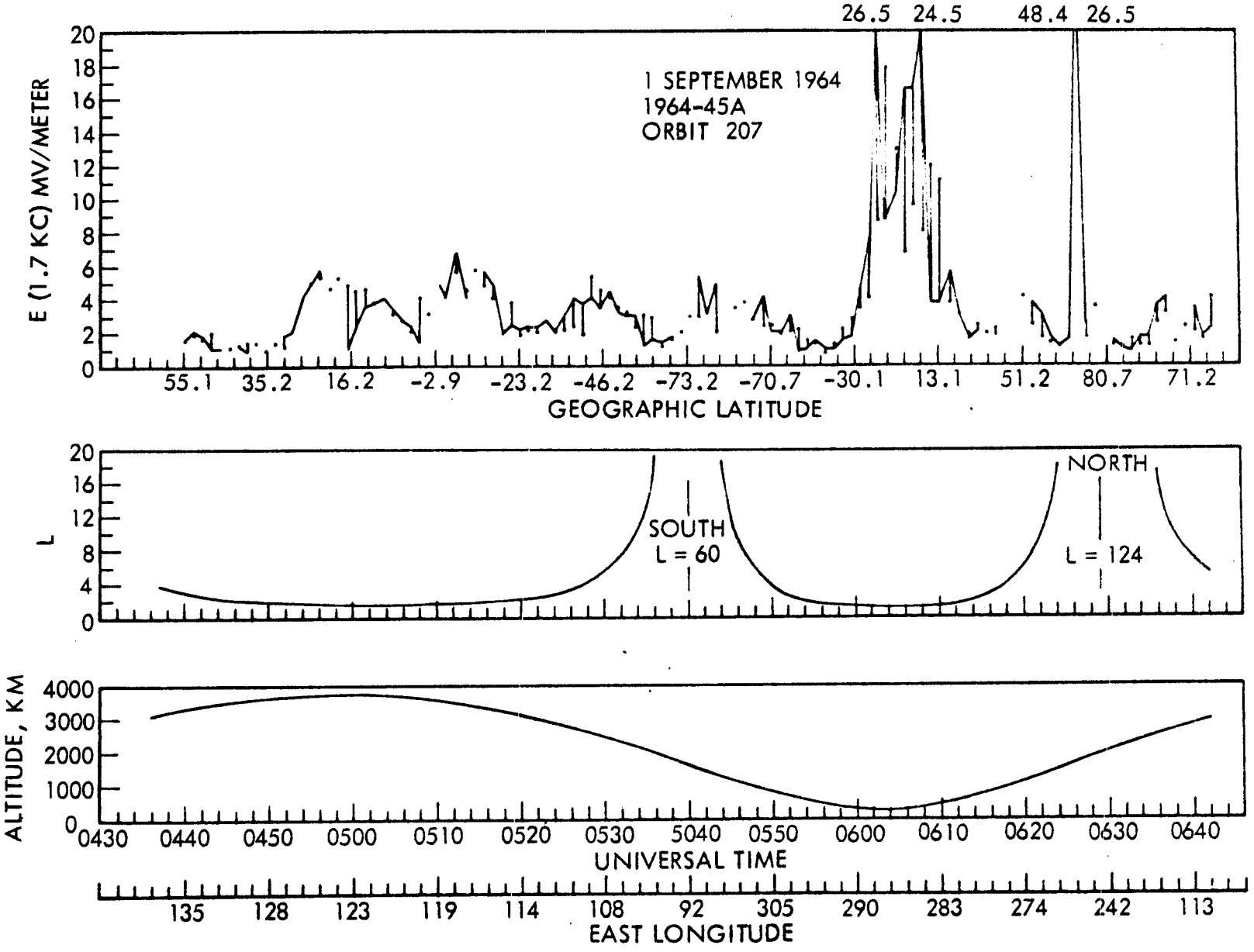

Figure 24. Data for orbit number 207 in same format as Figure 2 but no electron measurements are available.

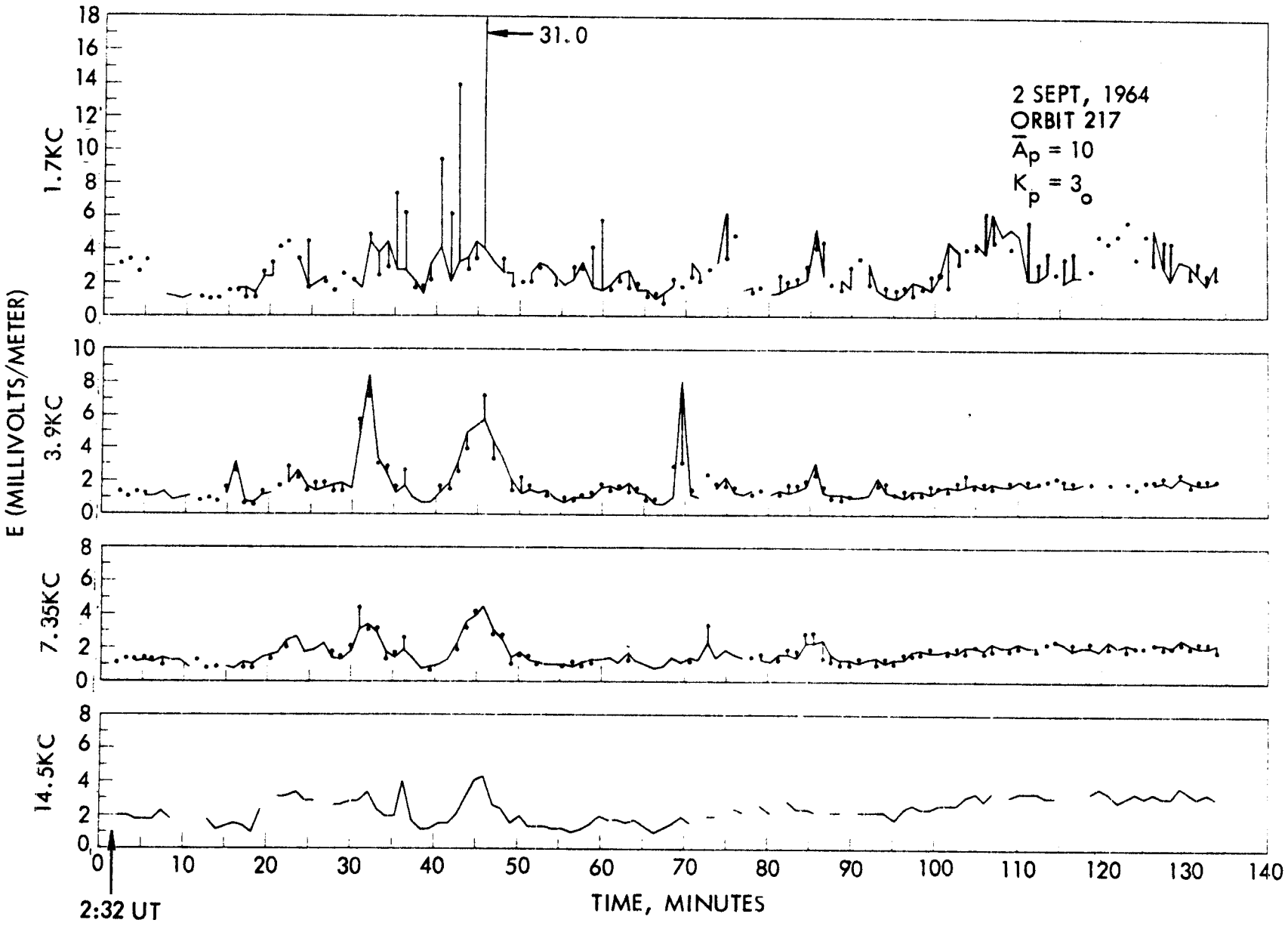

Figure 25. Data for orbit number 217 in same format as Figure 1.

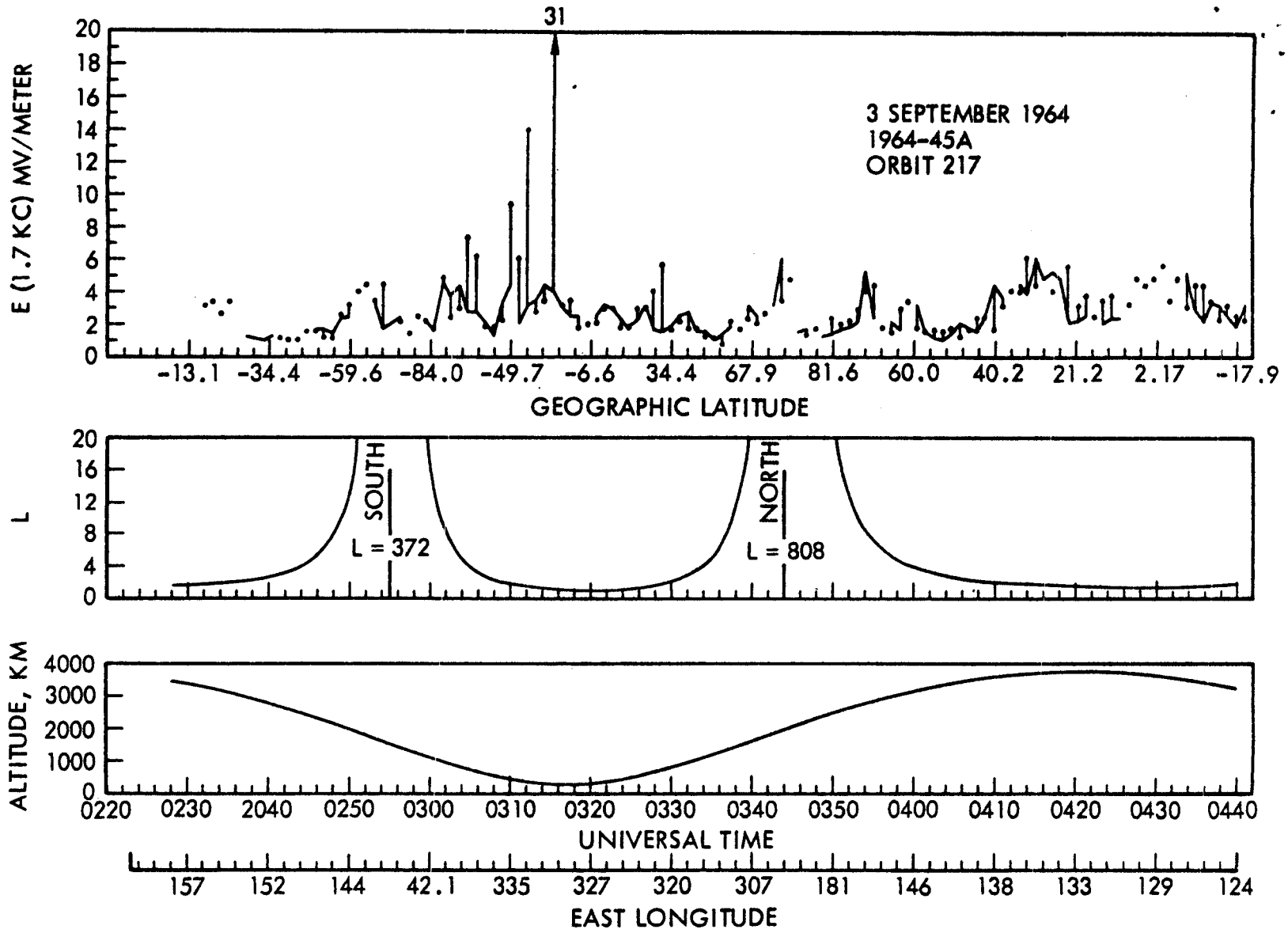

Figure 26. Data for orbit number 217 in same format as Figure 2 but no electron measurements are available.

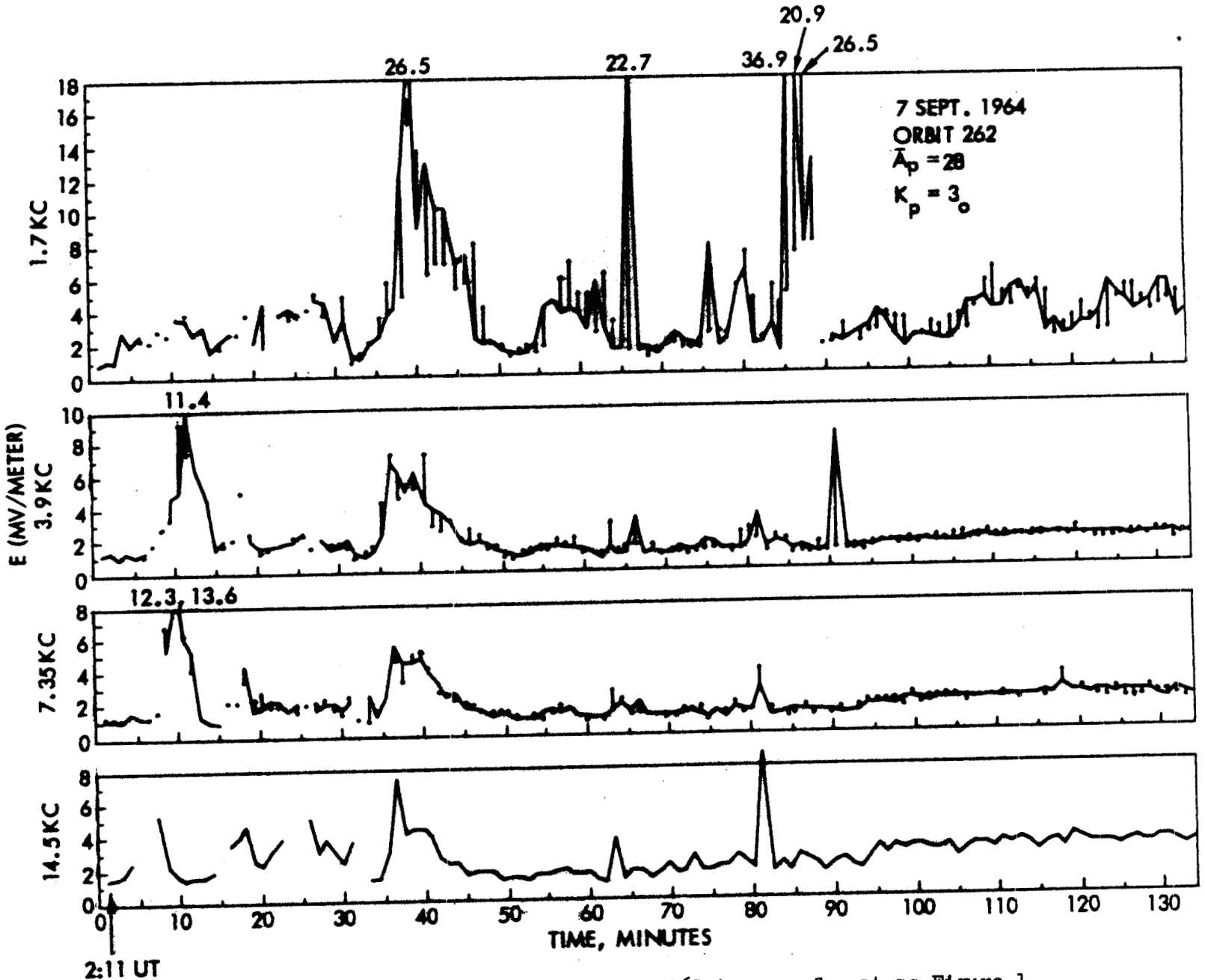

Figure 27. Data for orbit number 262 in same format as Figure 1.

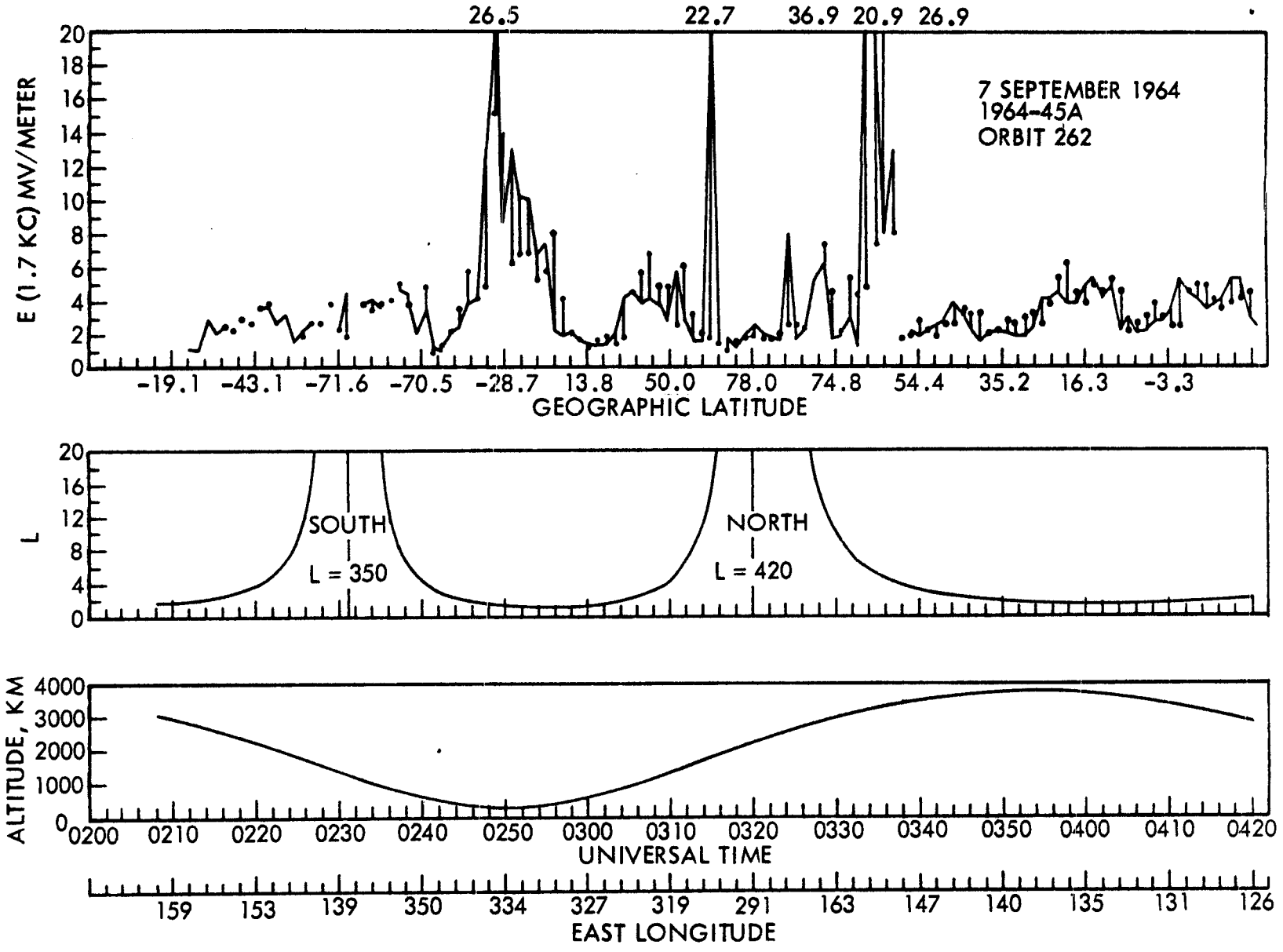

Figure 28. Data for orbit number 262 in same format as Figure 2 but no electron measurements are available.

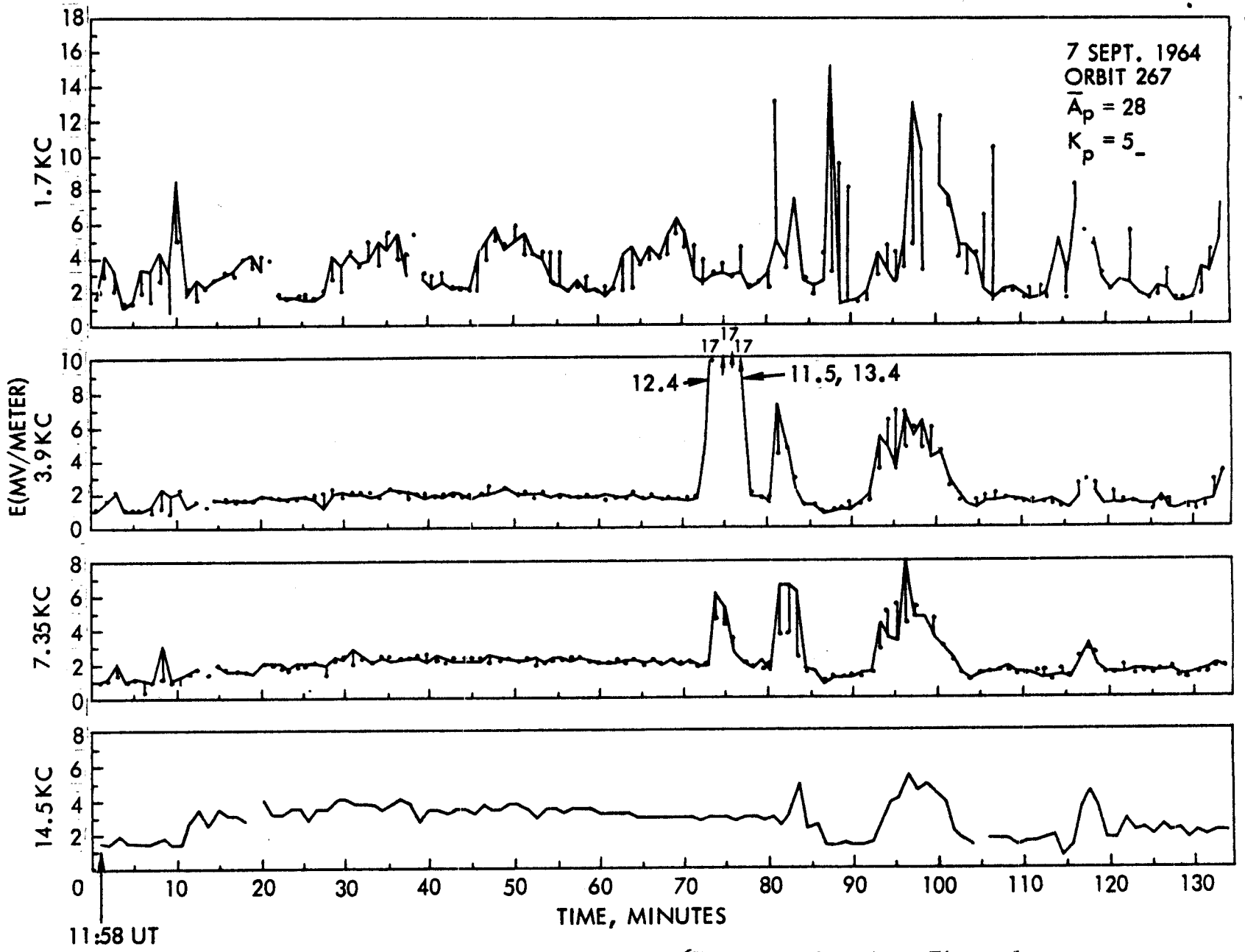

Figure 29. Data for orbit number 267 in same format as Figure 1.

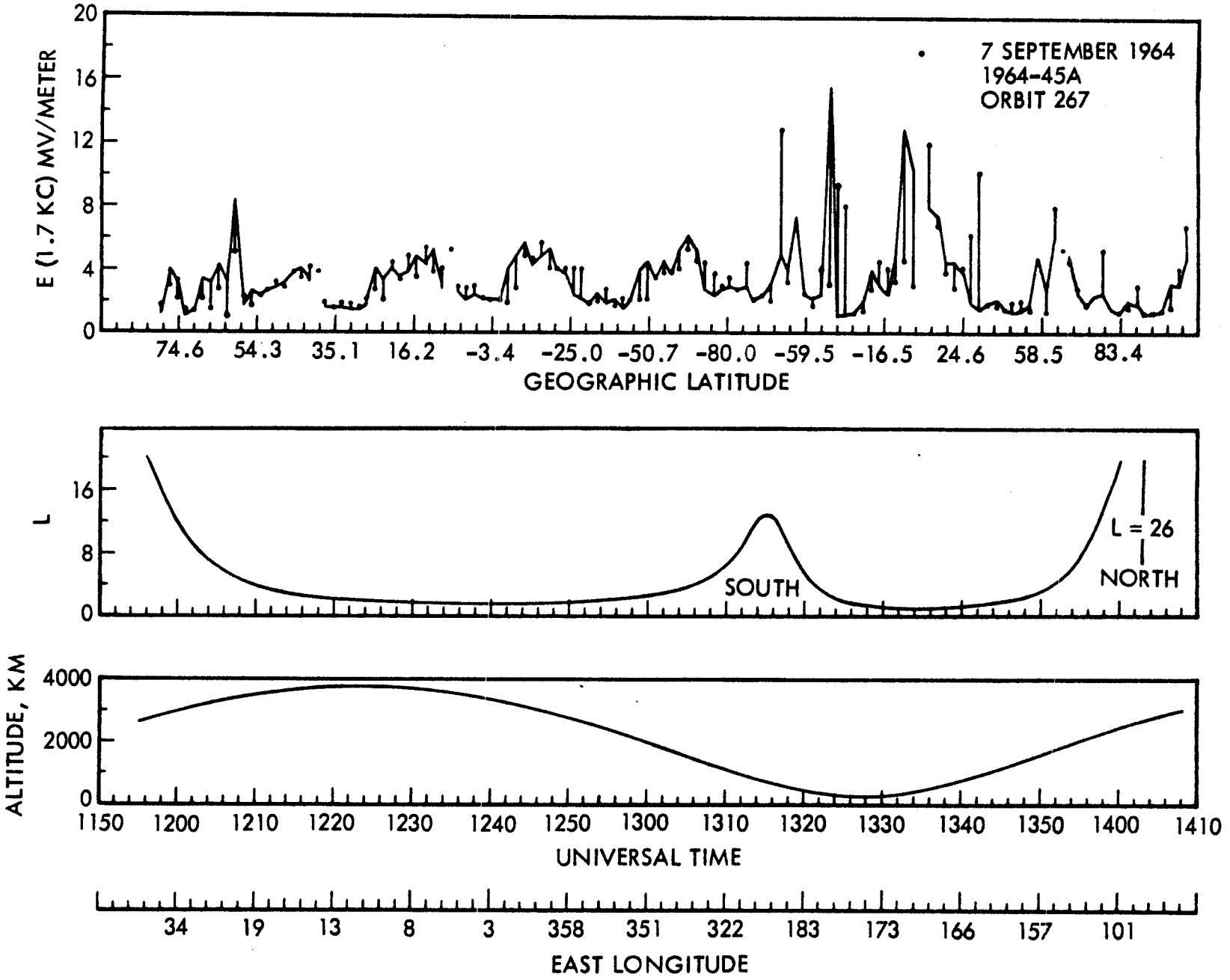

Figure 30. Data for orbit number 267 in same format as Figure 2 but no electron measurements are available.

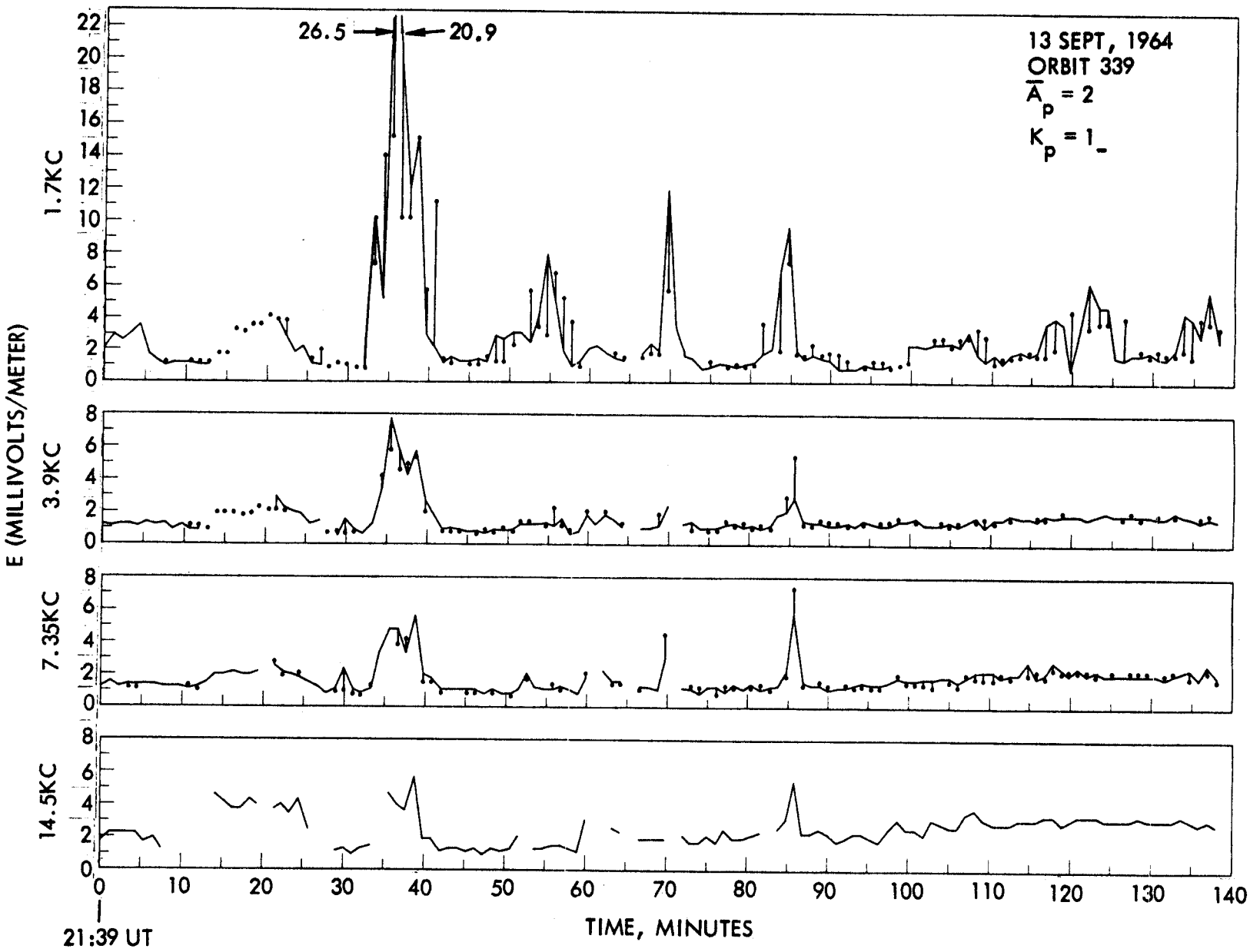

Figure 31. Data for orbit number 339 in same format as Figure 1.

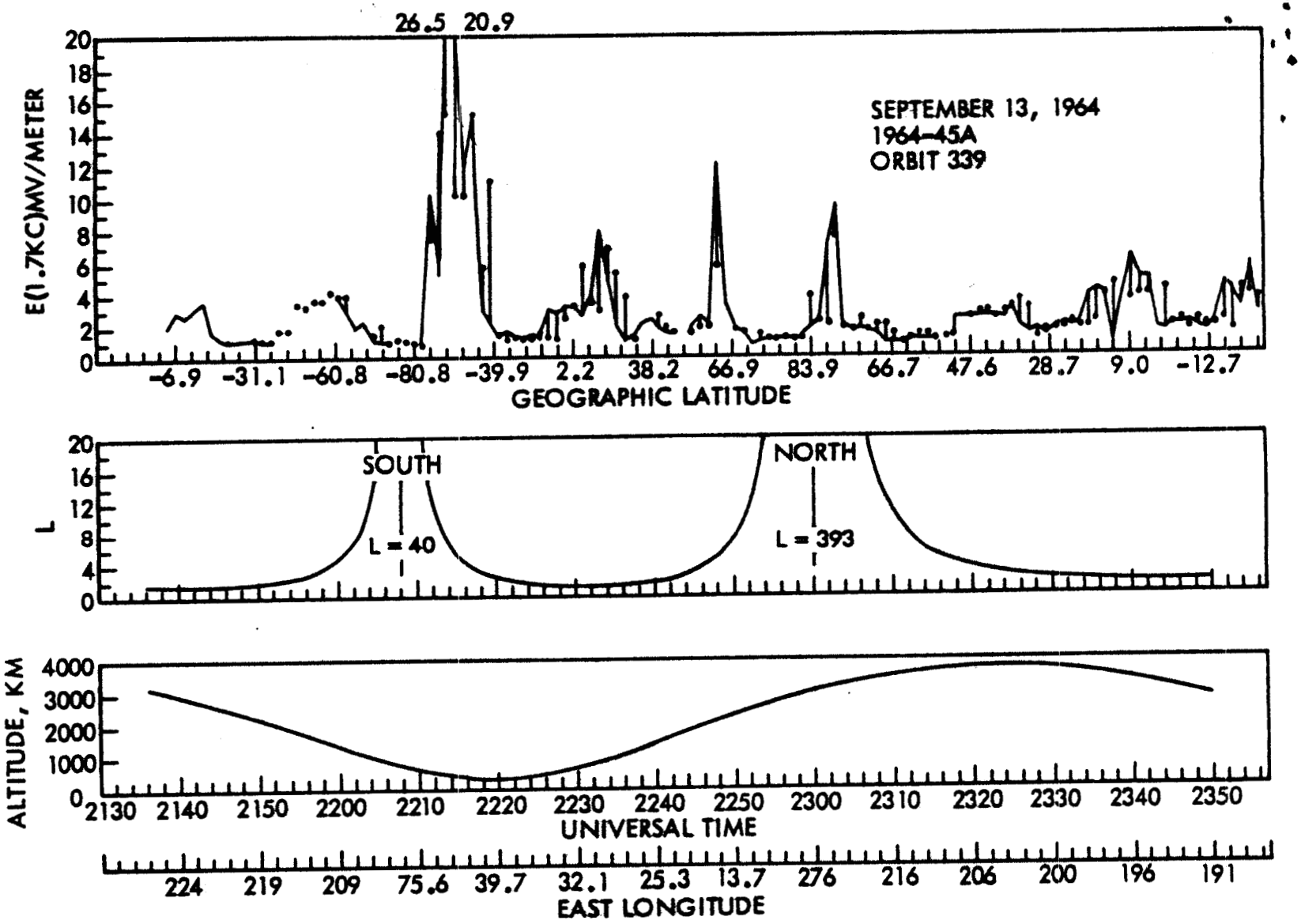

Figure 32. Data for orbit number 339 in same format at Figure 2 but no electron measurements are available.